Kaon Femtoscopy at High Baryon Density
paper proposal

Li'Ang Zhang, Bijun Fan
liangzhang@mails.ccnu.edu.cn
Central China Normal University

Motivation

1. Femtoscopy is a technique, that relates momentum correlations between particles to the their emission region and final state interaction (FSI).
2. Correlation function in Astronomy:

$$C\left(\vec{d}\right) = \frac{\langle I_1 I_2 \rangle}{\langle I_1 \rangle \langle I_2 \rangle} = 1 + \left| \int \rho(\vec{r}) e^{i(\overrightarrow{k_1} - \overrightarrow{k_2}) \cdot \vec{r}} d^3 r \right|^2$$

$$q_{inv} = |p_1^{\mu} - p_2^{\mu}|$$
$$k^* = \frac{q_{inv}}{2}$$

3. Correlation function in particle physics

$$C(k^*) = 1 + \int S(\vec{r}^*) \left[\left| \psi(\vec{k}^*, \vec{r}^*) \right|^2 - 1 \right] d^3 r^* = \frac{P(p_1^*, p_2^*)}{P(p_1^*) P(p_1^*)} = \frac{Same(q_{inv})}{Mix(q_{inv})}$$

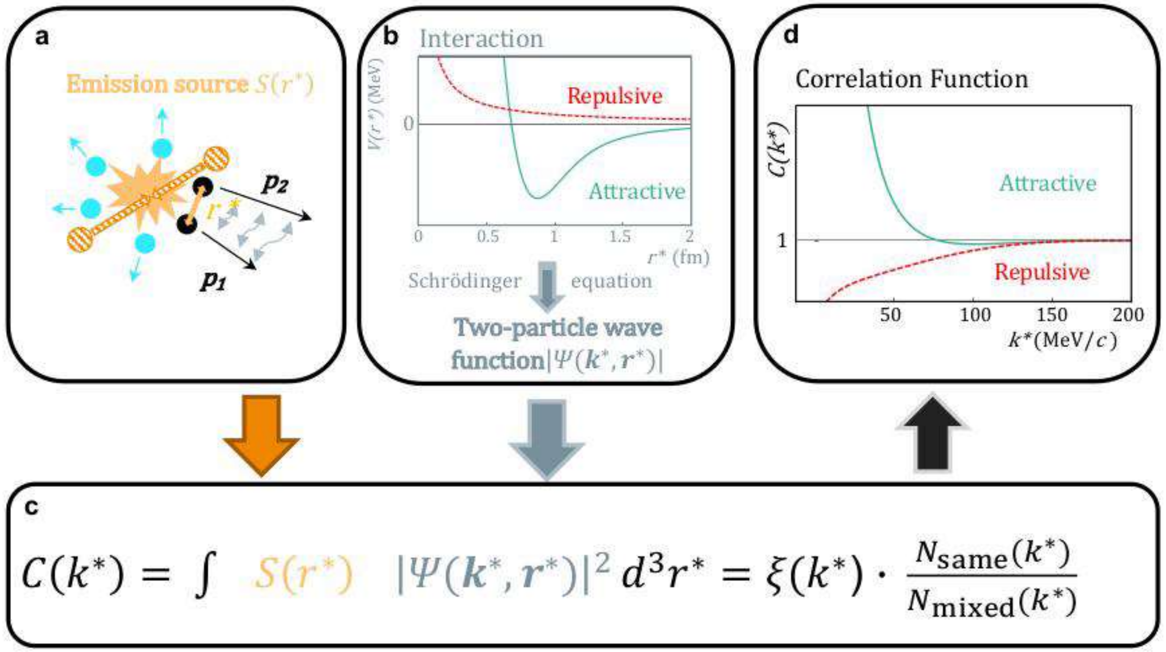

It is particularly interesting to study the dependence on the collision energy because freeze-out condition depends on energy.

1. Kaon-kaon correlation functions is an important supplement to that of pions, as they are less affected by resonance decays and has hadronic cross section.
2. Neutral kaon correlation function can also provide the final state interaction information.

Correlation function

1. The Lednický parameterization incorporates quantum statistics with strong FSI. FSI arise in the $K_s^0 - K_s^0$ channels due to the near-threshold resonances, $a_0(980)$ and $f_0(980)$.

$$CF(q) = 1 + \lambda\left(e^{[-R_{inv}^2 q_{inv}^2]} + \frac{1-\epsilon^2}{2}\left[\left|\frac{f(k^*)}{R_{inv}}\right|^2 + \frac{4Re[f(k^*)]}{\sqrt{\pi}R_{inv}}F_1(q_{inv}R_{inv}) - \frac{2Im[f(k^*)]}{R_{inv}}F_2(q_{inv}R_{inv})\right]\right)$$

- λ - the correlation strength; R_{inv} - the size of the particle-emitting source; ϵ - $K^0\overline{K}^0$ abundance asymmetry
- $f(k^*)$ is the s-wave scattering amplitude for a given system

$$f(k^*) = \frac{1}{2}[f_0(k^*) + f_1(k^*)],\ f_I(k^*) = \frac{\gamma_r}{m_r - s - i\gamma_r k^* - i\gamma_r' k_r'}$$

- m_r - the mass of the resonances; γ_r - the couplings parameters of the resonances

2. Sinyukov-Bowler method for K^+K^+ correlation function:

$$C(q_{inv}) = N[(1-\lambda) + K_{coul}(q_{inv}, R)\lambda(e^{[-R_{inv}^2 q_{inv}^2]} + 1)]$$

- λ - the correlation strength; R_{inv} - the size of the particle-emitting source; N – normalize factor; $K_{coul}(q_{inv}, R)$ - coulomb factor

General information

1. Paper title:

   Energy dependence of Kaon correlation function in high baryon density region

2. PAs:

   Wensong Cao, Bijun Fan, Youquan Qi, Li'Ang Zhang, Xin Dong, Chuan Fu, Xiaofeng Luo, Shusu Shi, Yaping Wang, Nu Xu, Yingjie Zhou

3. PA representatives:

   Bijun Fan (K^+K^+ CF), Li'Ang Zhang($K_s^0K_s^0$ CF)

4. Target Journal: PRL/PLB
5. Webpage: https://drupal.star.bnl.gov/STAR/blog/lazhang/WebPage-Energy-dependence-Kaon-correlation-function-high-baryon-density-region
6. Analysis note: https://www.overleaf.com/read/mxhtjbwsdygy#33cacb (ongoing)
7. Paper draft: preparation

Relative presentation

$K_s^0K_s^0$:
https://drupal.star.bnl.gov/STAR/system/files/20220721CFPWG_LiAngZhang.pdf
https://drupal.star.bnl.gov/STAR/system/files/20220913_LiAngZhang_FXTK0sK0sCF.pdf
https://drupal.star.bnl.gov/STAR/system/files/20230301LiAngUpdateAndPaperProposal_v3.pdf
https://drupal.star.bnl.gov/STAR/system/files/20230425LiAngK0s-K0sCFUpdate.pdf
https://drupal.star.bnl.gov/STAR/system/files/20230629STARBESIIWorkshop_LiAngZhang_BijunFan.pdf
https://drupal.star.bnl.gov/STAR/system/files/20230803LiAngK0s-K0sCFUpdate.pdf
https://drupal.star.bnl.gov/STAR/system/files/K0sK0sCFUpdates_LiAngZhang_PreliminaryRequest.pdf
https://drupal.star.bnl.gov/STAR/system/files/K0sK0sA0F0Par_LiAngZhang.pdf
K^+K^+ :
https://drupal.star.bnl.gov/STAR/system/files/K_CF_0.pdf
https://drupal.star.bnl.gov/STAR/system/files/sys_K_CF_6.pdf
https://drupal.star.bnl.gov/STAR/system/files/KK_CF_3GeV_0.pdf
https://drupal.star.bnl.gov/STAR/system/files/collaboration%20meeting_0.pdf
https://drupal.star.bnl.gov/STAR/system/files/KK_CF_FXT_3p85_Collabration_meeting_bijunFan.pdf
https://drupal.star.bnl.gov/STAR/system/files/KK_3p2GeV_CF_0525_pwg.pdf
https://drupal.star.bnl.gov/STAR/system/files/deltaphistar_3p2_KK.pdf
https://drupal.star.bnl.gov/STAR/system/files/preliminary_request_3p2_KK_230601_0.pdf
https://drupal.star.bnl.gov/STAR/system/files/Preliminary_request_KK_HBT_3p2to3p9_Bijun_230810_v2.pdf
https://drupal.star.bnl.gov/STAR/system/files/Collabration_meeting_KK_HBT_FXT_Bijun_231017sss.pdf
https://drupal.star.bnl.gov/STAR/system/files/Charged_Kaon_HBT_STAR_FXT_with_eTOF_0111.pdf

Abstract

Kaons are less affected by resonance decays and have smaller hadronic cross-sections. Comparing to that of pions, they could provide a more direct view of the particle-emitting source. In this paper, we present the first measurements of the $K^+ - K^+$, $K_s^0 - K_s^0$ femtoscopic correlations from Au + Au collisions at $\sqrt{s_{NN}}$ = 3.0, 3.2, 3.5, 3.9, and 4.5 GeV, measured by the STAR experiment at RHIC.

The Kaon correlation functions as function of relative momentum q_{inv} are analyzed in one-dimension due to limited event statistics. For comparison, pion correlation functions are also studied with the same fashion. Extracted radius parameter r_G and correlation strength λ are consistent between charged Kaon and neutral-Kaon within uncertainties and show no clear energy dependence while both Kaon's r_G and λ are lower than that of pion's. Unlike observed at higher collision energies, the measured Kaon source size parameters do not follow the m_T-scaling extracted from pion correlation functions at the same collisions. In addition, it is observed that the K^0 abundance asymmetry is decreased as a function of collision energy. The results of the transport mode UrQMD calculations qualitatively describe the measured results.

Data set

System	Trigger ID	Production tag	Library tag	V_z	V_r	events
3.0 GeV	620052	P19ie	SL20	198~202 cm	$V_x^2 + (V_y + 2)^2 < 2.25\ or\ 4\ cm$	~260 M
3.2 GeV	680001	P21id/P23id	SL21d/SL23d			~206 M
3.5 GeV	720000	P23ie	SL23e			~111 M
3.9 GeV	730000	P21id/P23ie	SL21d/SL23e			~100 M
4.5 GeV	740000, 740010	P21id/P23ie	SL21d/SL23e		$(V_x + 0.3)^2 + (V_y + 2)^2 < 2.25\ or\ 4\ cm$	~124 M

System	0-5%	5-10%	10-20%	20-30%	30-40%	40-50%	50-60%	60-70%	70-80%
3.0 GeV	https://drupal.star.bnl.gov/STAR/system/files/Sweger_3p0GeV_StandardNewest_fcv2020Nov11.pdf								
3.2 GeV	https://drupal.star.bnl.gov/STAR/system/files/Centrality_Determination_for_3_2_GeV_2019_Production.pdf								
3.5 GeV	https://drupal.star.bnl.gov/STAR/blog/eloyd/Run-20-35GeVFXT-Centrality-Definition								
3.9 GeV	https://drupal.star.bnl.gov/STAR/blog/eloyd/Run-20-39GeVFXT-Centrality-Definition								
4.5GeV	https://drupal.star.bnl.gov/STAR/blog/eloyd/Run-20-45GeVFXT-Centrality-Definition								

Systematic uncertainty calculation

1. Statistical uncertainty: $\Delta\sigma = \sqrt{\left|\sigma_{default}^2 - \sigma_{varied}^2\right|}$
2. Systematic difference: $\Delta\mathrm{CF} = \left|\mathrm{CF}_{default} - \mathrm{CF}_{varied}\right|$
3. Final sys. Error: $\mathrm{sys.err} = \sqrt{\Delta\mathrm{CF}^2 - \Delta\sigma^2}$
4. Take sys. Error = 0 when $\Delta\sigma > \Delta\mathrm{CF}$
5. One systematic source different cut: $\sqrt{(\mathrm{sys.err}_1^2 + \cdots + \mathrm{sys.err}_n^2)/n}$
6. Different systematic source: add in quadrature

Systematic uncertainty

$K^+ - K^+$	Default	Variation
NHitsFit	>15	>17, 19
DCA	< 3 cm	< 2.5, < 2.0
$\|n\sigma\|$	< 3	< 2.5, < 2.0
$\|\Delta\phi^*\|$	> 0.05	0.04, > 0.045, > 0.055, > 0.06
$\|\Delta\theta\|$	>0.02	>0.015, >0.025
Splitting level	-0.5 < SL < 0.6	-0.5 < SL < 0.5, -0.5 < SL < 0.7
TOF m^2	$0.16 < m^2 < 0.36$	$0.2 < m^2 < 0.32$ GeV^2/c^4
Fitting range	0.00-0.2	0.00-0.16, 0.00-0.25, 0.02-0.2
Momentum correction	corrected	Not corrected

$K_S^0 - K_S^0$	Default	Variation
NHitsFit	>10 (>15 for 3.0 GeV)	> 15, 20 (>17, 20 for 3.0 GeV)
$\chi^2_{prim\ \pi^\pm}$	>10 (>13 for 4.5 GeV)	>7, 13 (>10, 16 for 4.5 GeV)
χ^2_{NDF}	<3 (<5 for 3.0 GeV)	<4, 5 (<3, 4 for 3.0 GeV)
χ^2_{Topo}	<3 (<5 for 3.0 GeV)	<4, 5 (<3, 4 for 3.0 GeV)
Mass window	2σ	3σ, 4σ
Side Band range	[0.42~0.48]⊕[0.52~0.58]	[0.41~0.49]⊕[0.51~0.59], [0.43~0.47]⊕[0.53~0.57]
Background estimate method	Side band	rotation
Fitting range (only 3.0 GeV)	w/ first point	w/o first point
Normalize Range	0.5-0.7	0.55-0.75, 0.45-0.65
Momentum correction	corrected	Not corrected

Systematic contribution @ 3.0 GeV

Other energies in backup

$K^+ - K^+$	r_G	λ
NHitsFit	0	0
DCA	0.40%	0.35%
$\|n\sigma\|$	3.32%	0
$\|\Delta\phi^*\|$	0.91%	0.90%
$\|\Delta\theta\|$	0	0
Splitting level	0.03%	0.22%
TOF m^2	0	0
Momentum correction	0.83%	0.39%
Fit range	2.20%	0
total	4.19%	1.06%

$K_s^0 - K_s^0$	r_G	λ	ϵ
NHitsFit	0	0	0
$\chi^2_{prim\ \pi^\pm}$	0	0	46.72%
χ^2_{NDF}	0	10.99%	0
χ^2_{Topo}	0	0	9.75%
Mass window	0	7.66%	0
Side Band range	0	0	0
Background estimate method	0	0	28.28%
Fitting range	9.31%	29.73%	0
Normalize Range	0	0	0
Momentum correction	0	0	0
total	9.31%	32.61%	55.48%

Fig. 1

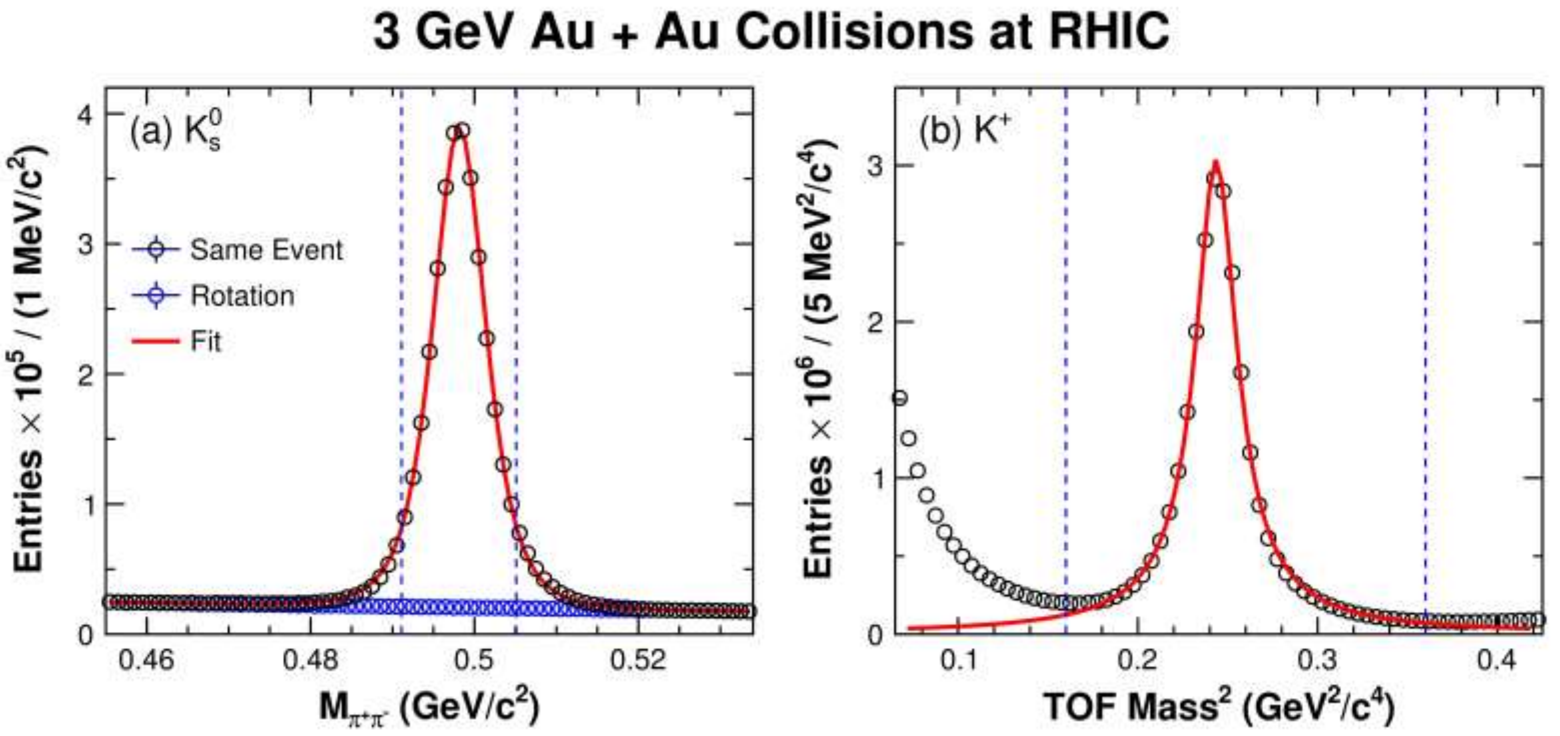

Fig. 1: Panel (a) shows the invariant mass distribution of K_s^0 from the combination pair of π^+ and π^-. Blue circles represent the background distribution constructed by rotating momentum vectors of daughter pions. Panel (b) is the square of mass distribution extracted from the time-of-flight(TOF) detector. Results of the fitting are shown by red line while the vertical blue dashed lines indicate the signal region.

Fig. 2

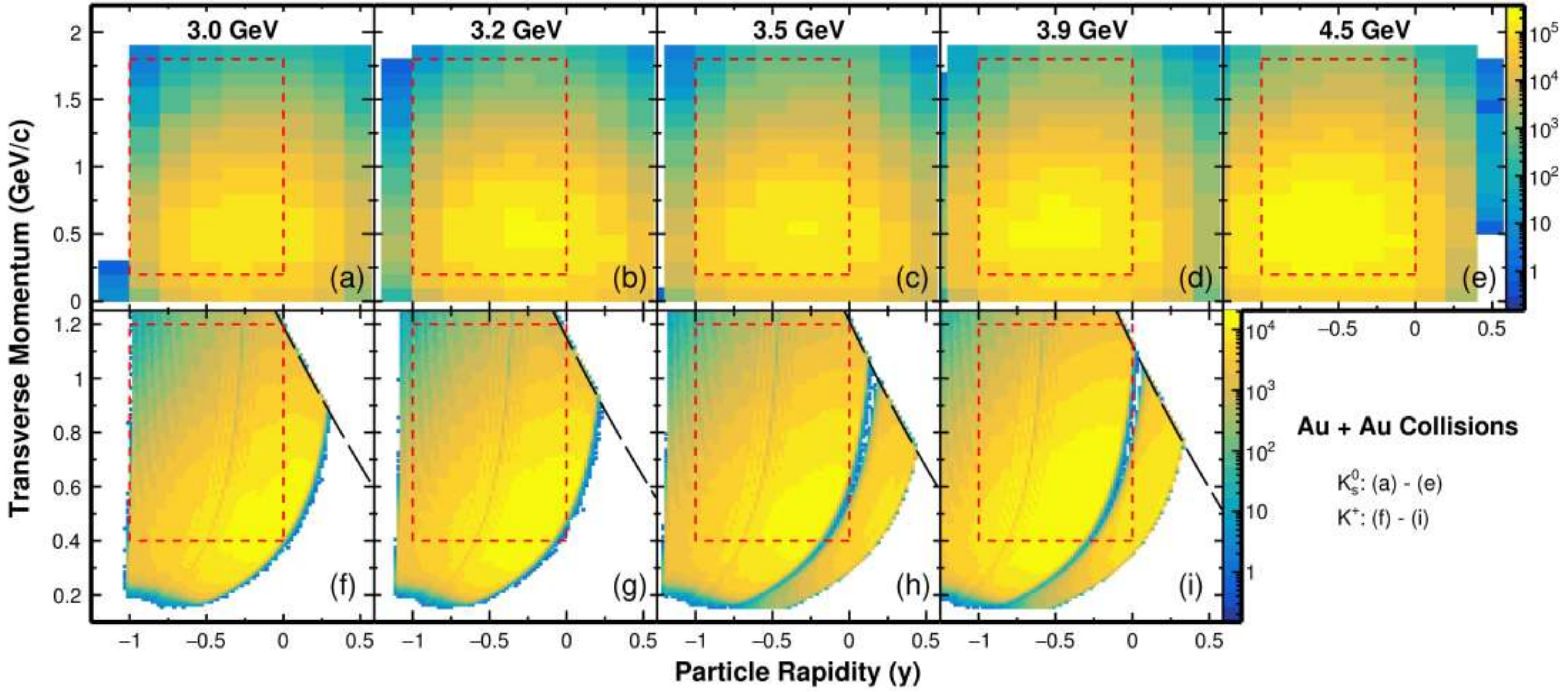

Fig. 2: K_S^0 (upper panels) and K^+ (lower panels) acceptances are shown as p_T vs. rapidity from $\sqrt{s_{NN}}$ = 3.0, 3.2, 3.5, 3.9 and 4.5 GeV Au+Au collisions. Dashed red boxes indicate the acceptance region used in the Kaon correlation function analysis. In the lower panels, the long dashed black lines show the momentum cuts of purity request, which limits the charged Kaon acceptance at mid-rapidity.

Fig. 3

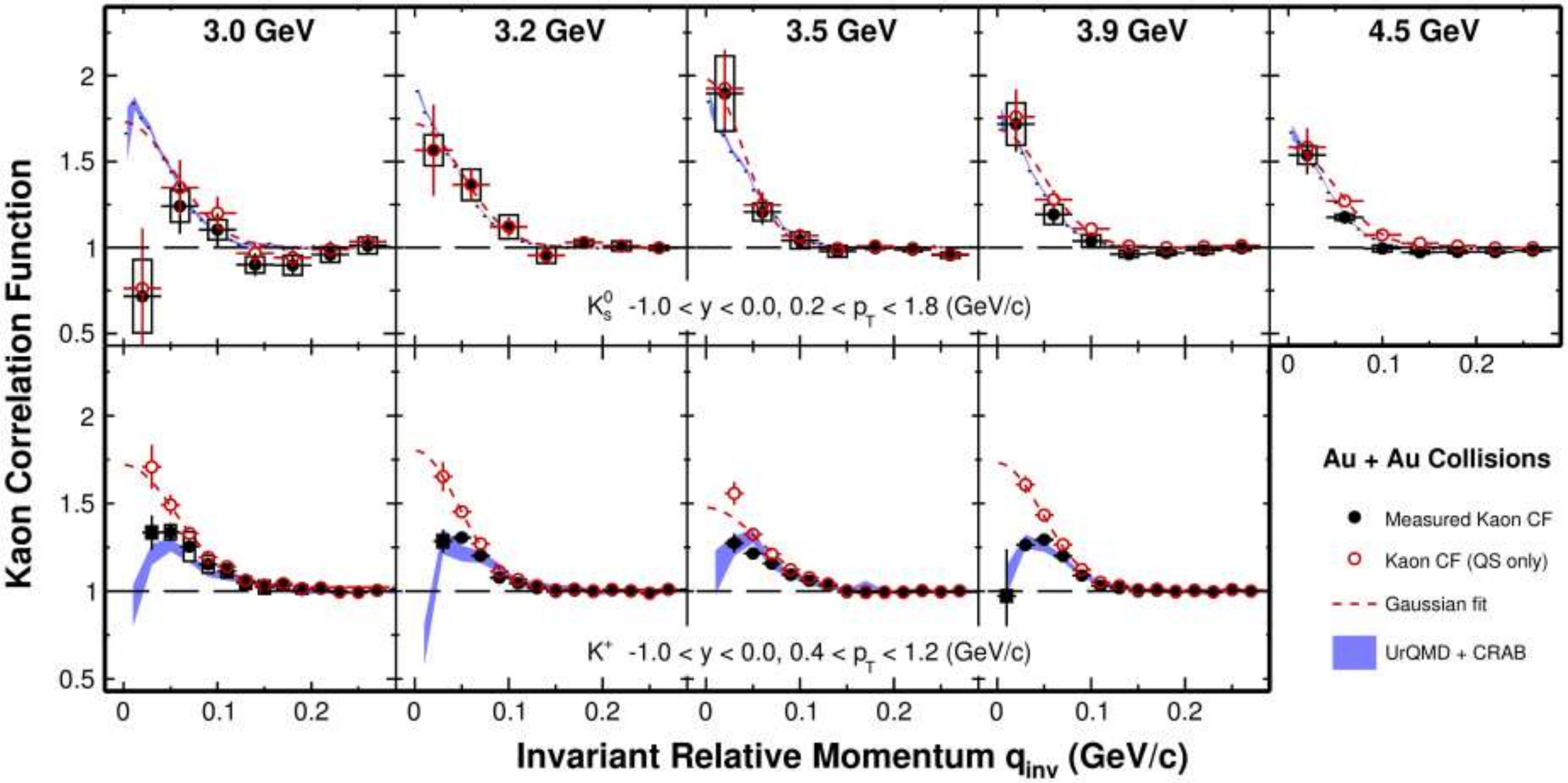

Fig. 3: One-dimension correlation functions of measured $K^0_s - K^0_s$ (upper panel) and $K^+ - K^+$ (lower panel) from $\sqrt{s_{NN}}$= 3.0, 3.2, 3.5, 3.9 and 4.5 GeV Au + Au collisions at 0-60% centrality. Vertical lines and open boxes represent the statistical and systematic uncertainties, respectively. Open circles show the Kaon correlation function with the effect of only quantum statistics, and the results of a Gaussian source to the correlation function are shown by the dashed lines. The blue bands are Kaon correlation functions from transport model UrQMD plus a correlation package CRAB.

Fig. 4

[1]Phys. Lett. B 831, 137152 (2022)

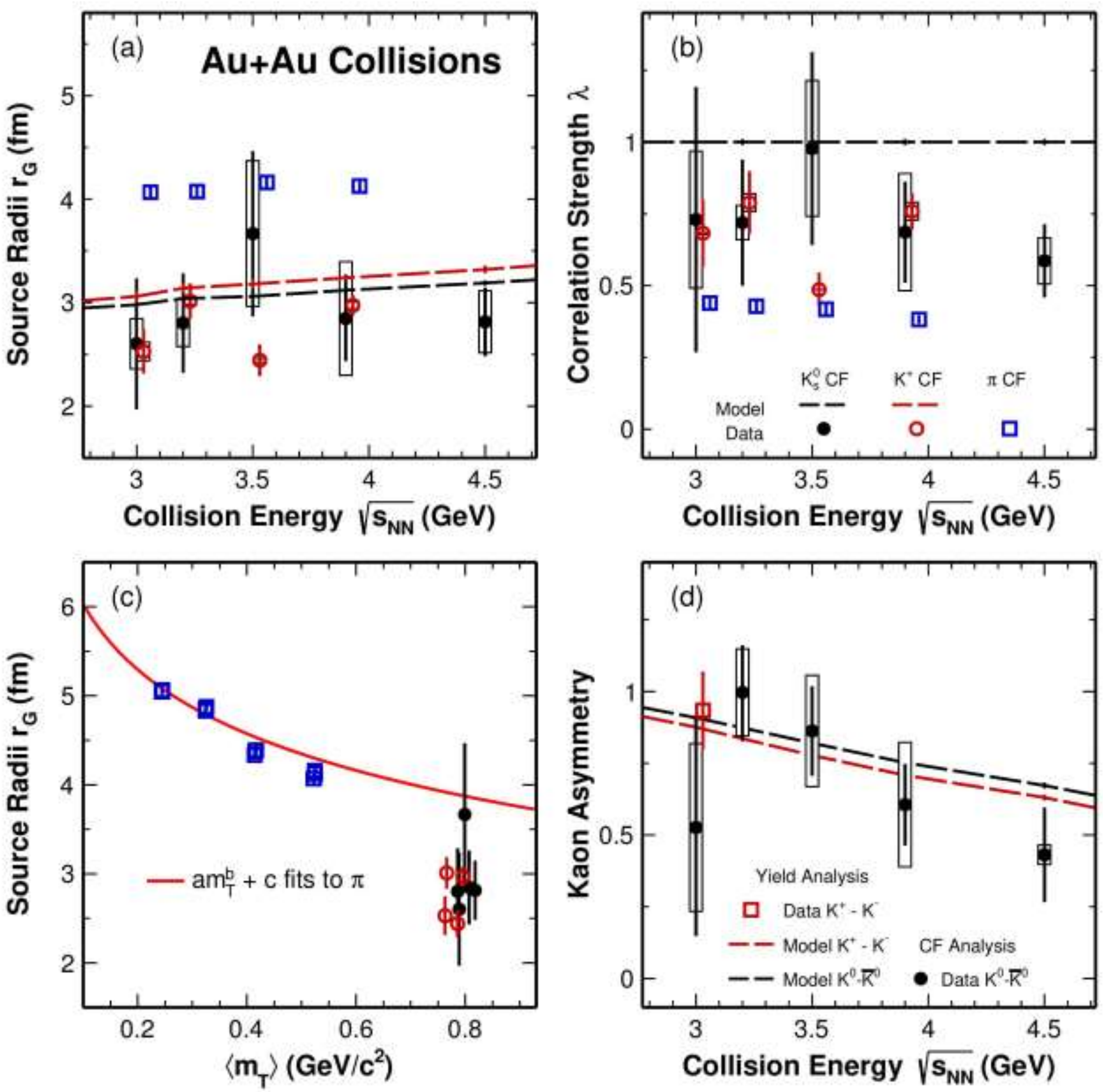

Fig. 4: Energy dependence of the extracted Gaussian source parameters $\mathrm{r_G}$ (a), correlation strength λ (b) and abundance asymmetry for $\mathrm{K^+ - K^-}$[1] (open circle) and $\mathrm{K^0 - \overline{K}^0}$ (solid circle) (d). Panel (c) shows $\langle \mathrm{m_T} \rangle$ dependence of the $\mathrm{r_G}$. For comparison, averaged one-dimension Gaussian source parameters from $\pi^+ - \pi^+$ and $\pi^- - \pi^-$ correlation functions are shown in panel (a), (b) and (c) as open squares. Results from transport model UrQMD are shown as dashed lines.

Table 1

	Parameters	3.0 GeV	3.2 GeV	3.5 GeV	3.9 GeV	4.5 GeV
Avg. $\pi - \pi$	r_G (fm)	4.07±0.06	4.07±0.06	4.16±0.06	4.13±0.05	No Acc.
	λ	0.44±0.01	0.43±0.01	0.42±0.01	0.38±0.01	No Acc.
	$\langle m_T \rangle$ (GeV/c^2)	0.522	0.523	0.524	0.525	No Acc.
$K^+ - K^+$	r_G (fm)	2.53±0.20 ±0.09	3.01±0.16 ±0.03	2.44±0.14 0.02	2.97±0.09 ±0.03	No Acc.
	λ	0.68±0.11 ±0.00	0.79±0.10 ±0.03	0.49±0.05 0.00	0.75±0.06 ±0.03	No Acc.
	$\langle m_T \rangle$ (GeV/c^2)	0.763	0.766	0.786	0.796	No Acc.
$K_s^0 - K_s^0$	r_G (fm)	2.60±0.62 ±0.24	2.80±0.47 ±0.23	3.67±0.78 ±0.70	2.85±0.40 ±0.55	2.81±0.32 ±0.30
	λ	0.73±0.46 ±0.24	0.72±0.21 ±0.06	0.97±0.33 ±0.24	0.69±0.17 ±0.20	0.59±0.12 ±0.08
	ϵ	0.53±0.37 ±0.29	1.00±0.16 ±0.15	0.86±0.15 ±0.19	0.61±0.14 ±0.22	0.43±0.16 ±0.03
	$\langle m_T \rangle$ (GeV/c^2)	0.789	0.786	0.799	0.807	0.818

Summary:

We report the first results of energy dependence of kaon-kaon correlation function at $\sqrt{s_{NN}}$=3.0, 3.2, 3.5, 3.9 and 4.5 GeV Au+Au collisions (0-60% centrality) measured by the STAR experiment at RHIC.

By fitting with one-dimensional function, the source size parameter r_G and the strength parameter λ are extracted at each collision energy. One finds that, within uncertainties, both source size and correlation strength parameters are consistent for charged- and neutral-Kaons. Comparing with that of pion's, the values r_G of Kaons are smaller while the λ are found to be larger, implying a smaller interaction cross sections for Kaons in the hadronic dominant environment. All these parameters are flat at these energy range.

The m_T-scaling is seen from pion correlation functions due to collective expansion takes place in such collisions. However, the Kaon results seem not follow the scaling from pion correlation functions which may indicate no equilibrium amongst pions and Kaons at these collisions. In addition, the abundance asymmetry parameter of K^0 is also determined and they are decreasing as a function of the collision energy which is consistent with the pair production becomes more important at higher collision energies.

Hadronic transport model (UrQMD) plus afterburner (CRAB) calculations for Kaon reproduced all of the above observations. Those findings indicate that the property of the medium created in these collisions are dictated by the hadronic interactions in the high baryon region. Previous publications on collective flow, proton high moments, strange hadron productions have also reached similar conclusions.

Request PWGC review

Back up

Lednický & Lyuboshitz model

[1] eConfC020620, THAT06 (2002)
[2] Phys. Rev. D 63, 094007 (2001)
[3] Phys. Rev. D 68, 014006 (2003)
[4] Nucl. Phys. B 121, 514–530 (1977)

- the Lednický parameterization incorporates quantum statistics with strong FSI. FSI arise in the $K_s^0 K_s^0$ channels due to the near-threshold resonances,a_0(980) and f_0(980).

$$CF(q) = 1 + \lambda\left(e^{[-R_{inv}^2 q_{inv}^2]} + \frac{1-\epsilon^2}{2}\left[\left|\frac{f(q_{inv}/2)}{R_{inv}}\right|^2 + \frac{4Re[f(q_{inv}/2)]}{\sqrt{\pi}R_{inv}}F_1(q_{inv}R_{inv}) - \frac{2Im[f(q_{inv}/2)]}{R_{inv}}F_2(q_{inv}R_{inv})\right]\right)$$

λ - the correlation strength; R_{inv} - the size of the particle-emitting source; ϵ – abundance asymmetry

$$F_1(z) = \int_0^z dx\,\frac{\exp(x^2 - z^2)}{z},\ F_2(z) = \frac{1-\exp(-z^2)}{z},\ \epsilon = \frac{K^0 - \bar{K}^0}{K^0 + \bar{K}^0}$$

$f(2q_{inv})$ is the s-wave scattering amplitude for a given system

$$f(q_{inv}/2) = \frac{1}{2}[f_0(q_{inv}/2) + f_1(q_{inv}/2)]$$

	m_{f_0}	$\gamma_{f_0 K\bar{K}}$	$\gamma_{f_0 \pi\pi}$	m_{a_0}	$\gamma_{a_0 K\bar{K}}$	$\gamma_{a_0 \pi\eta}$
Antonelli [1]	0.973	2.763	0.5283	0.985	0.4038	0.3711
Achasov2001 [2]	0.996	1.305	0.2684	0.992	0.5555	0.4401
Achasov2003 [3]	0.996	1.305	0.2684	1.003	0.8365	0.4580
Martin [4]	0.978	0.792	0.1990	0.974	0.3330	0.2220

$$f_I(q_{inv}/2) = \frac{\gamma_r}{m_r - s - 2i\gamma_r q_{inv} - i\gamma_r' k_r'}$$

$$s = 4[m_K^2 + (q_{inv}/2)^2]$$

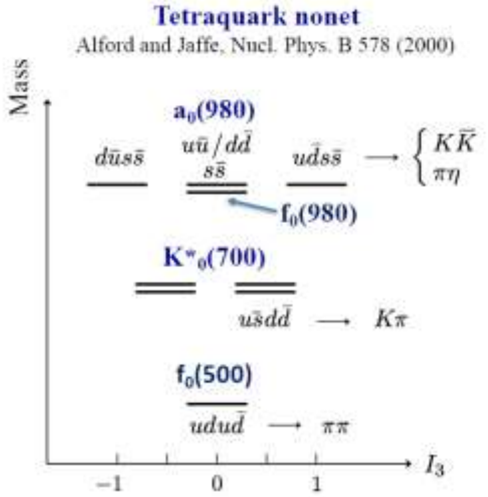

For f_0(980) the $k_r' = \sqrt{(q_{inv}/2)^2 + m_{K^0}^2 - m_\pi^2}$, for a_0(980) the $k_r' = \frac{\sqrt{m_\pi^4 + m_\eta^4 + s^2 - 2(m_\pi^2 m_\eta^2 + m_\pi^2 s + m_\eta^2 s)}}{2\sqrt{s}}$

Neutral kaon

- K^0 can change into a $\overline{K^0}$ through a second order weak interaction.
- $|K_{1,2}\rangle = \ 1/\sqrt{2}\,(|K^0\rangle \pm |\overline{K^0}\rangle)$
- $CP|K_{1,2}\rangle = \pm|K_{1,2}\rangle$
- $|K^0\rangle = 1/\sqrt{2}\,(|K_1\rangle + |K_2\rangle)$
- $K^0\ \overline{K^0}$ abundance asymmetry need to be considered at FXT energies

- Neglecting the effects of CP violation, the $|K_{1,2}\rangle$ are corresponding the K_s^0 and K_L^0

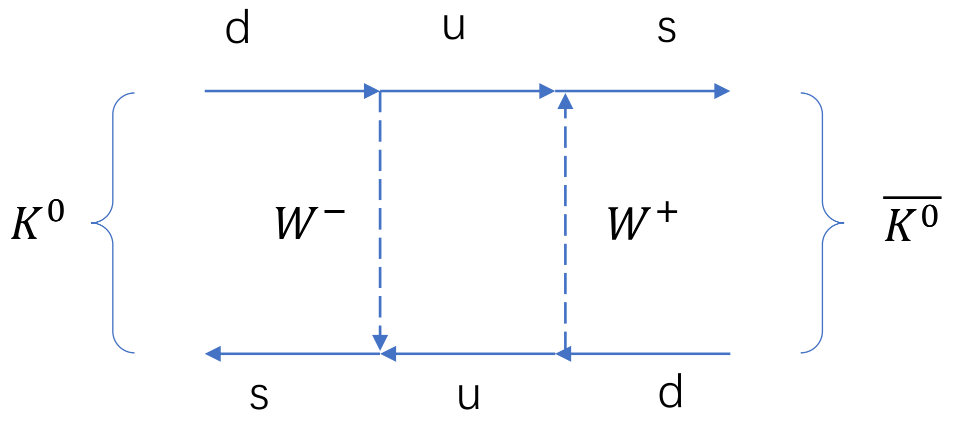

FSI of Kaon
$K^0K^0(\overline{K^0}\ \overline{K^0})$: QS
$K^0\ \overline{K^0}$: SI

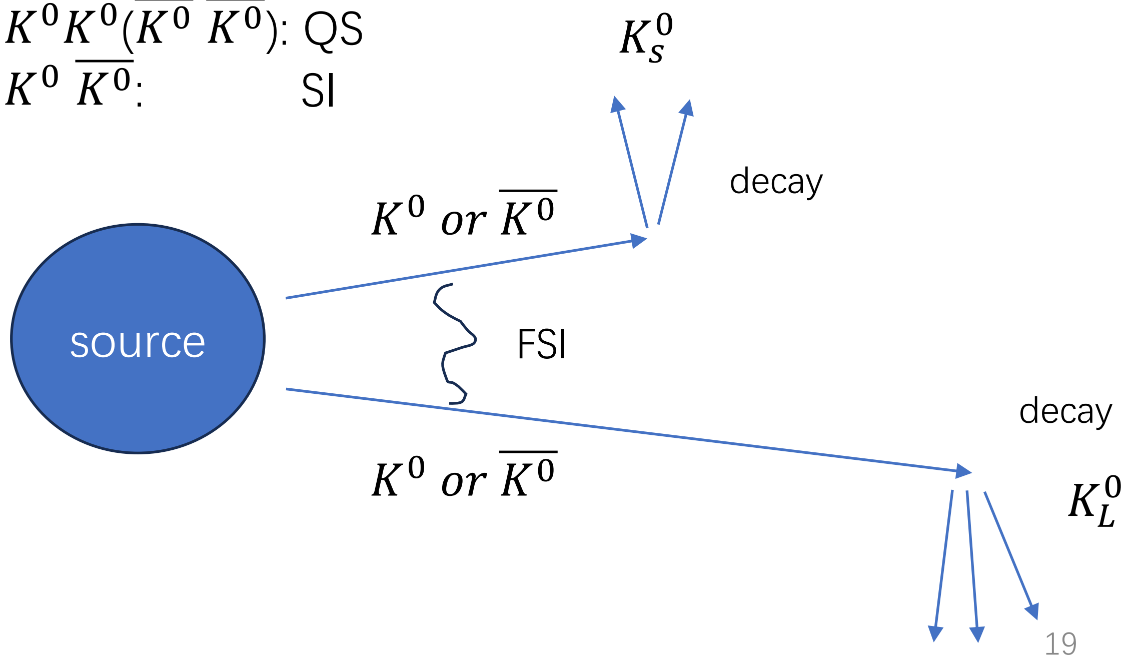

Systematic study

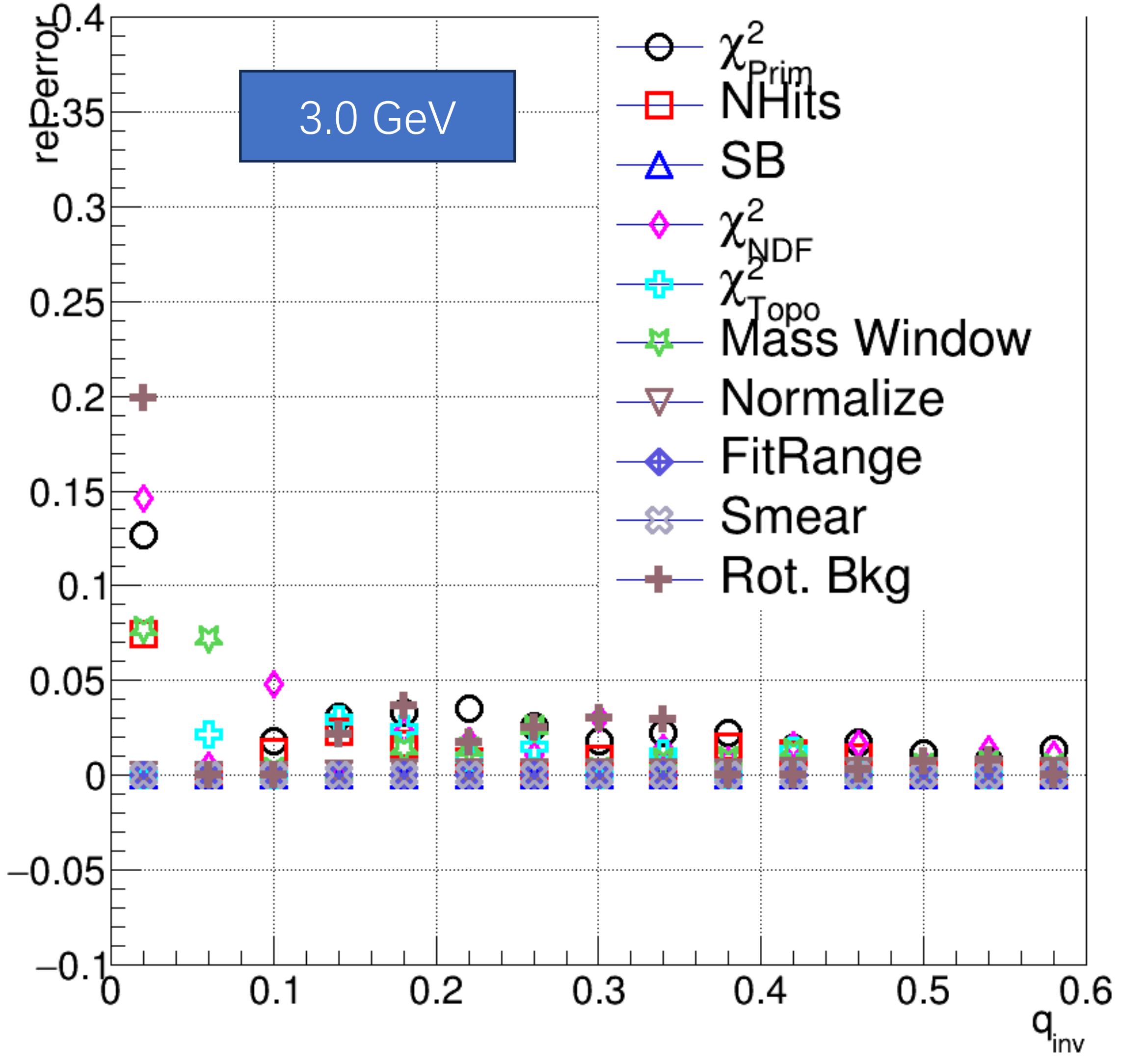

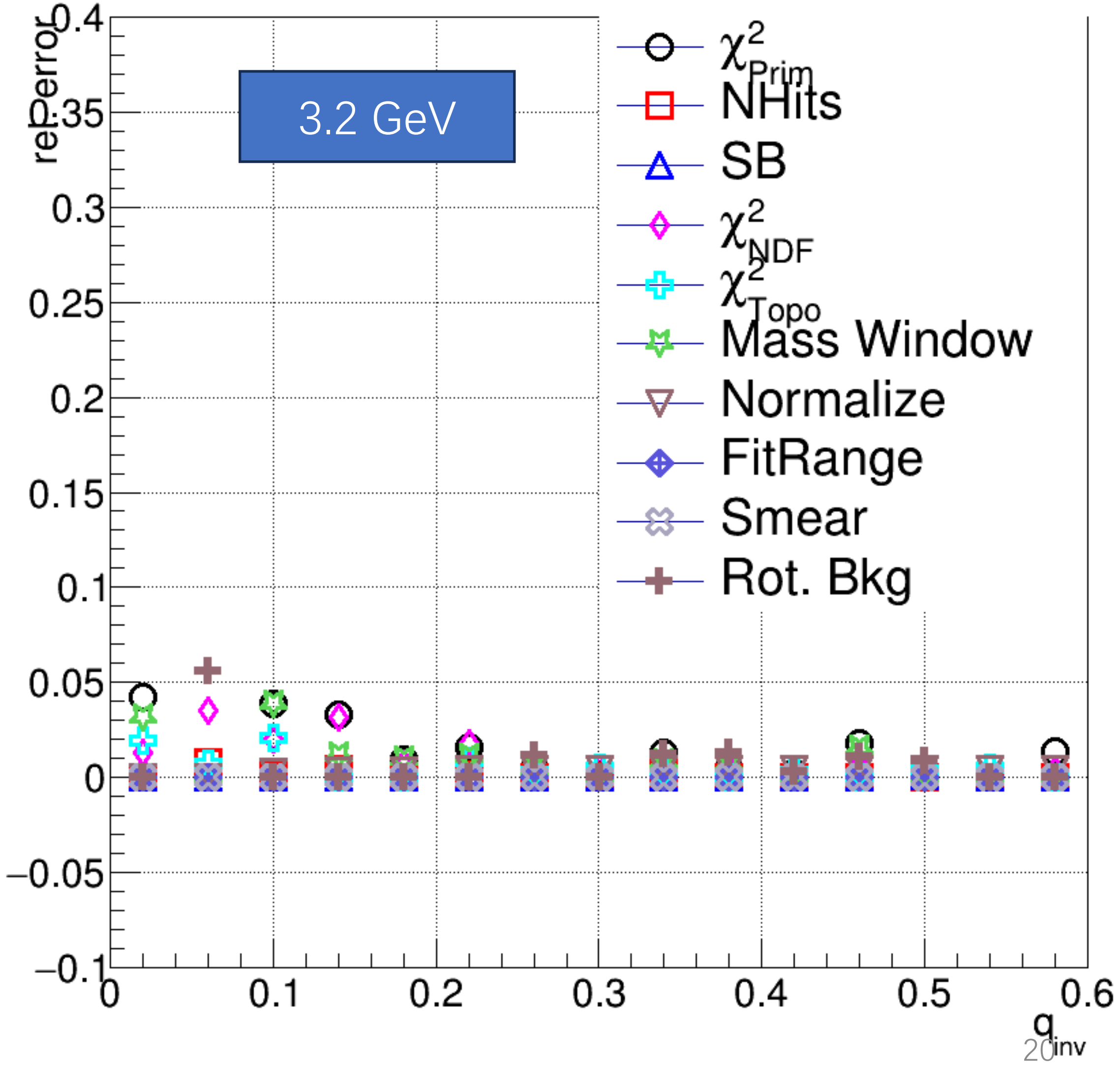

Systematic study

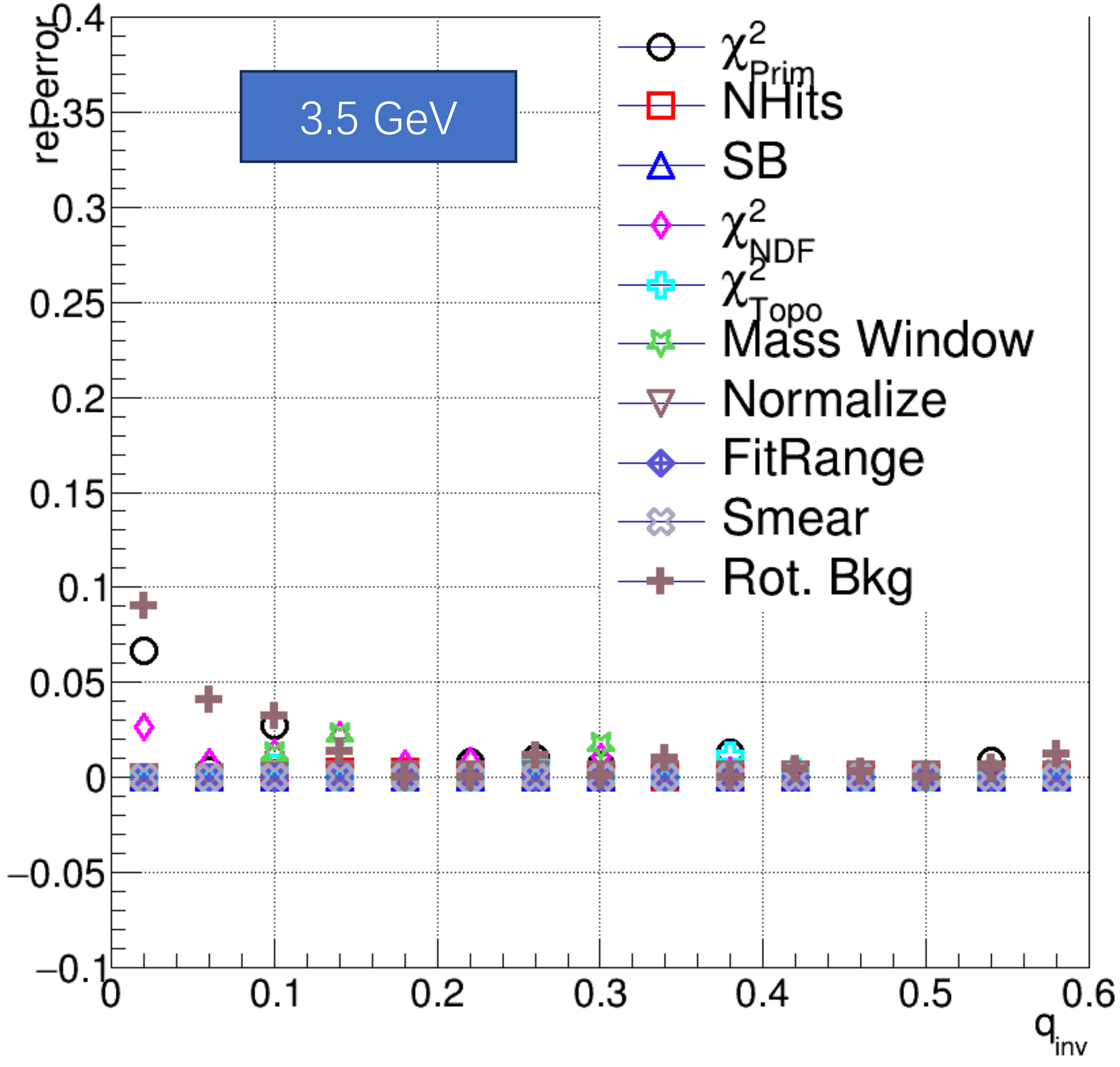

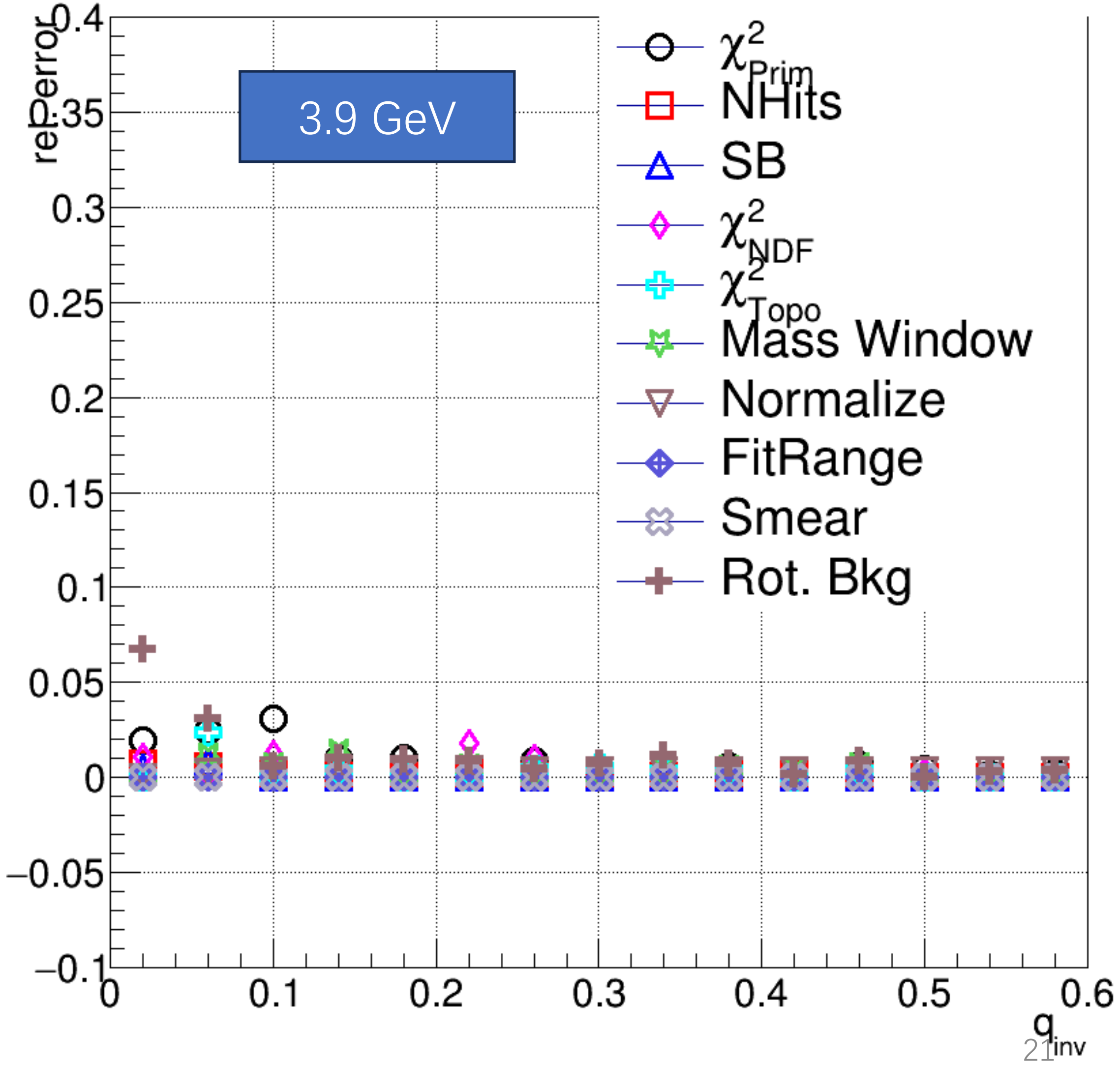

Systematic study

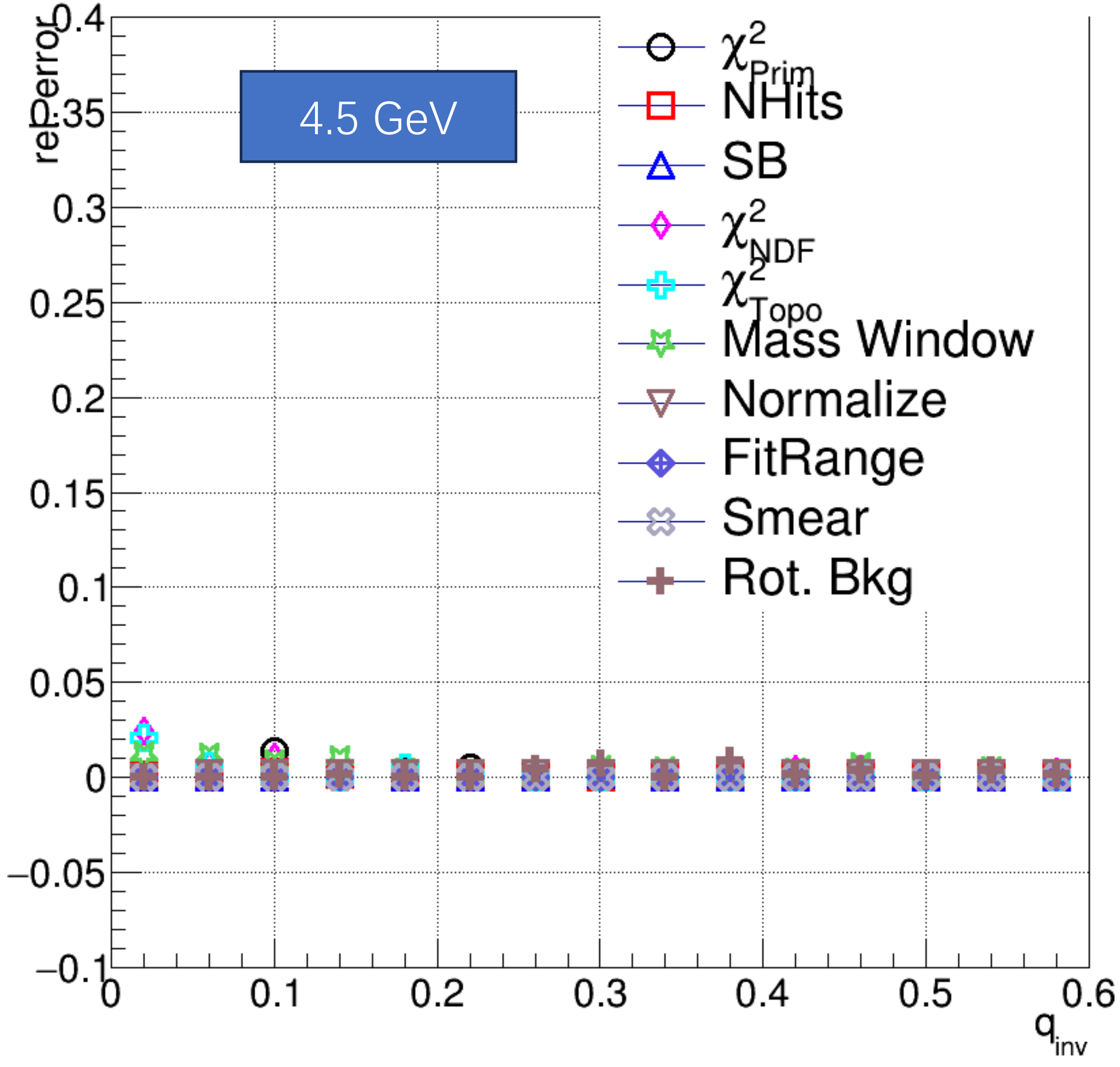

Systematic study

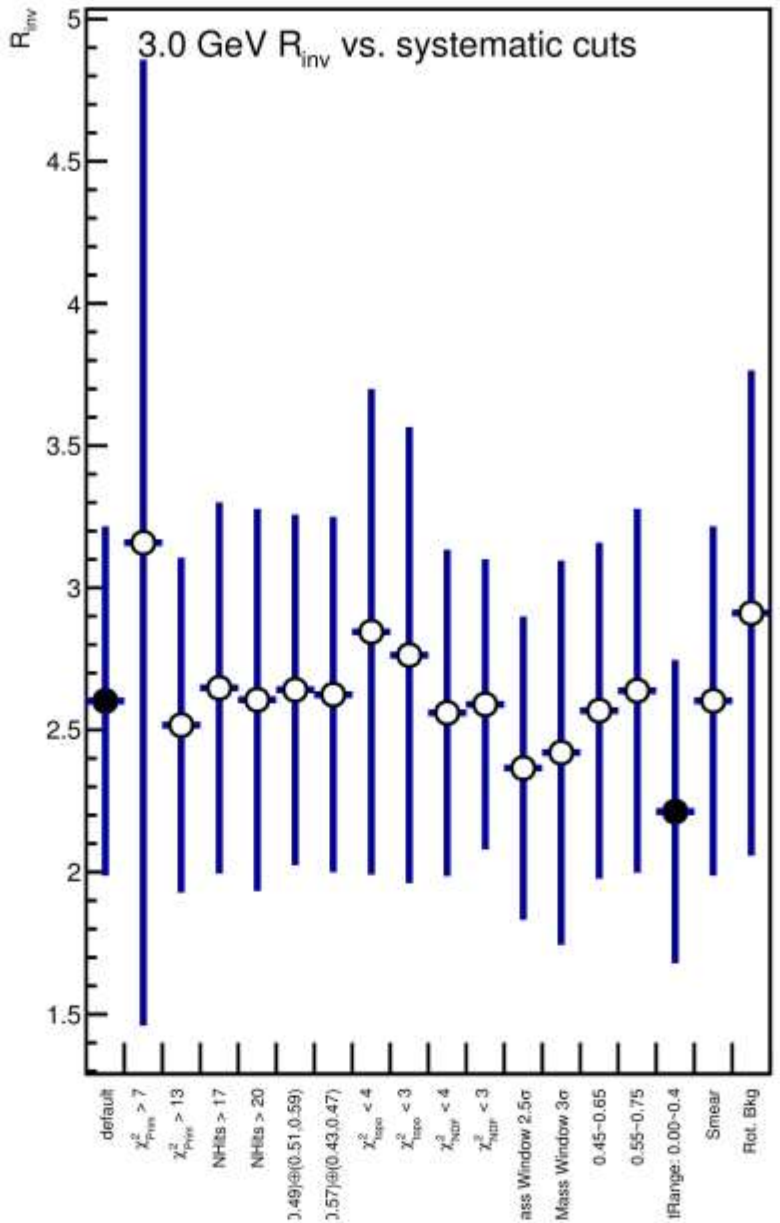

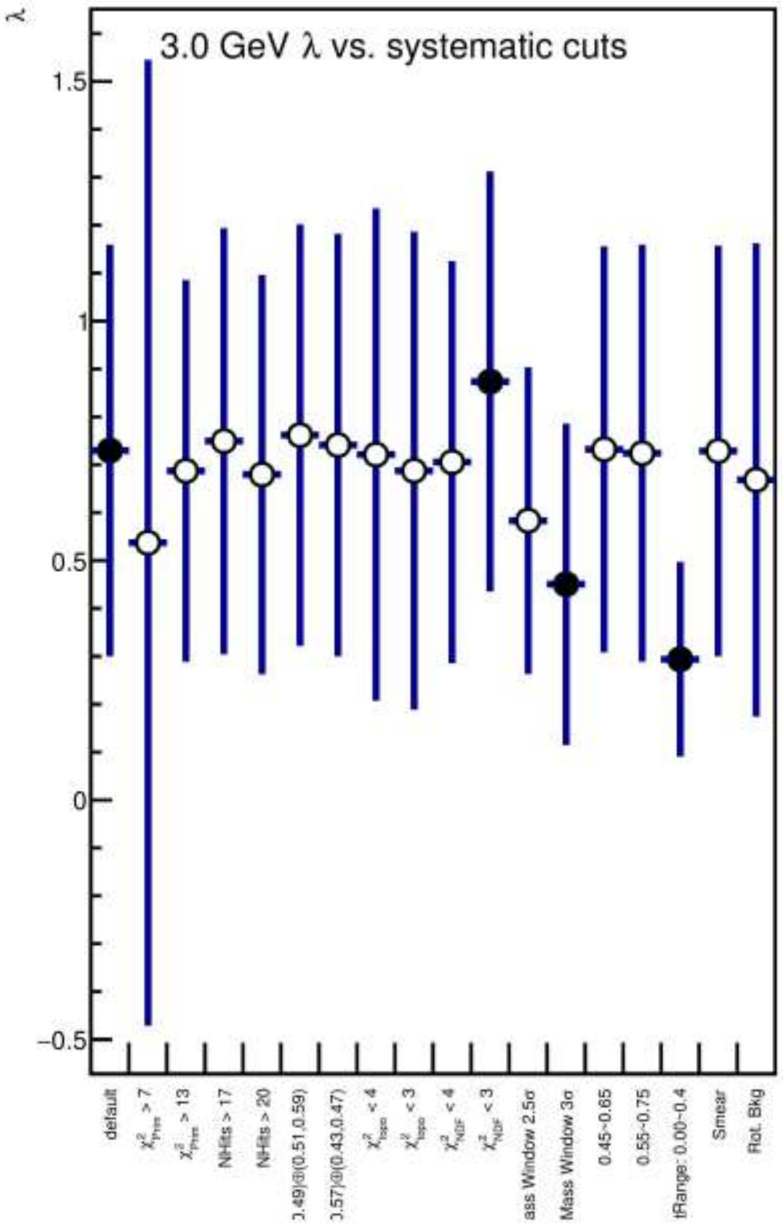

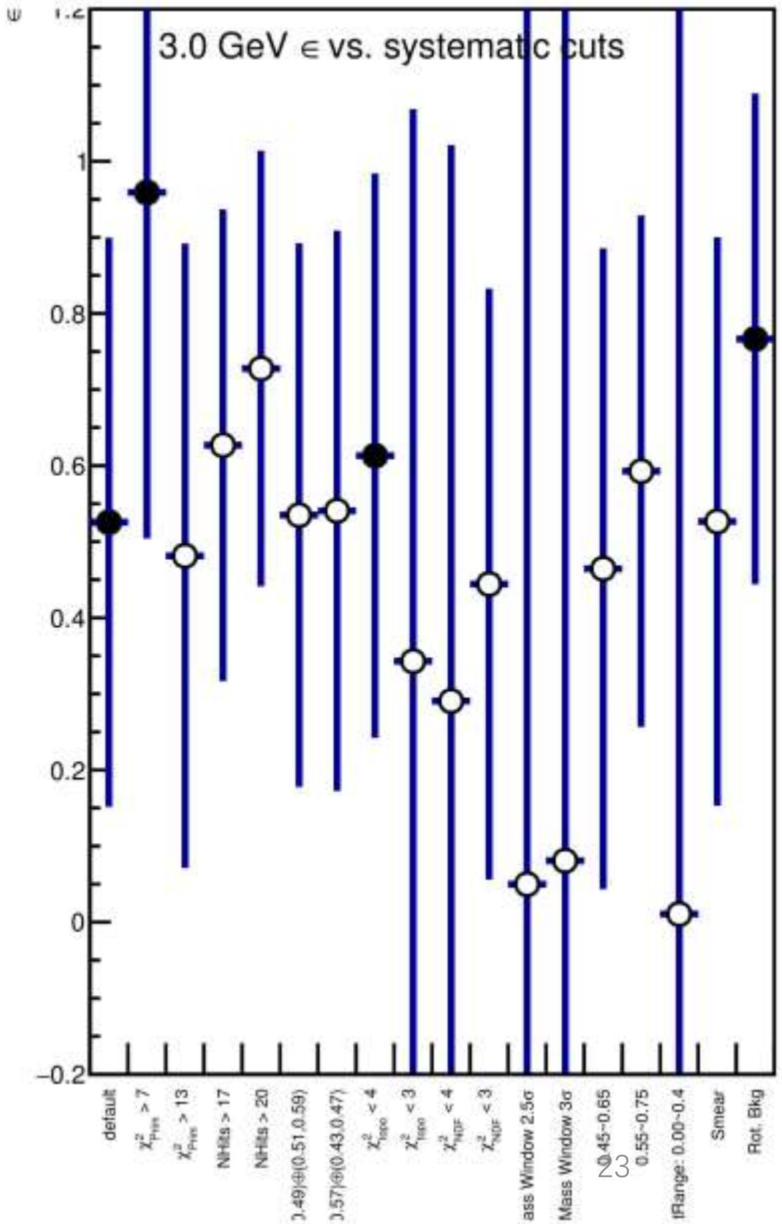

Systematic study

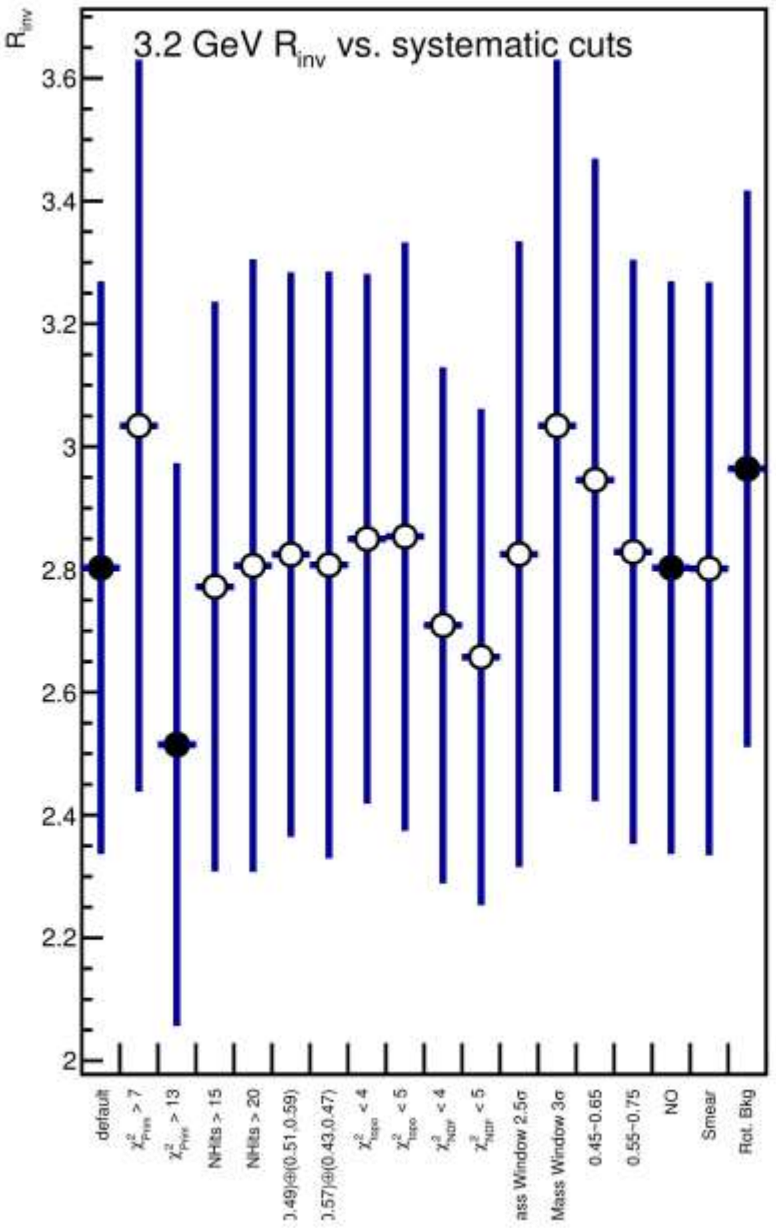

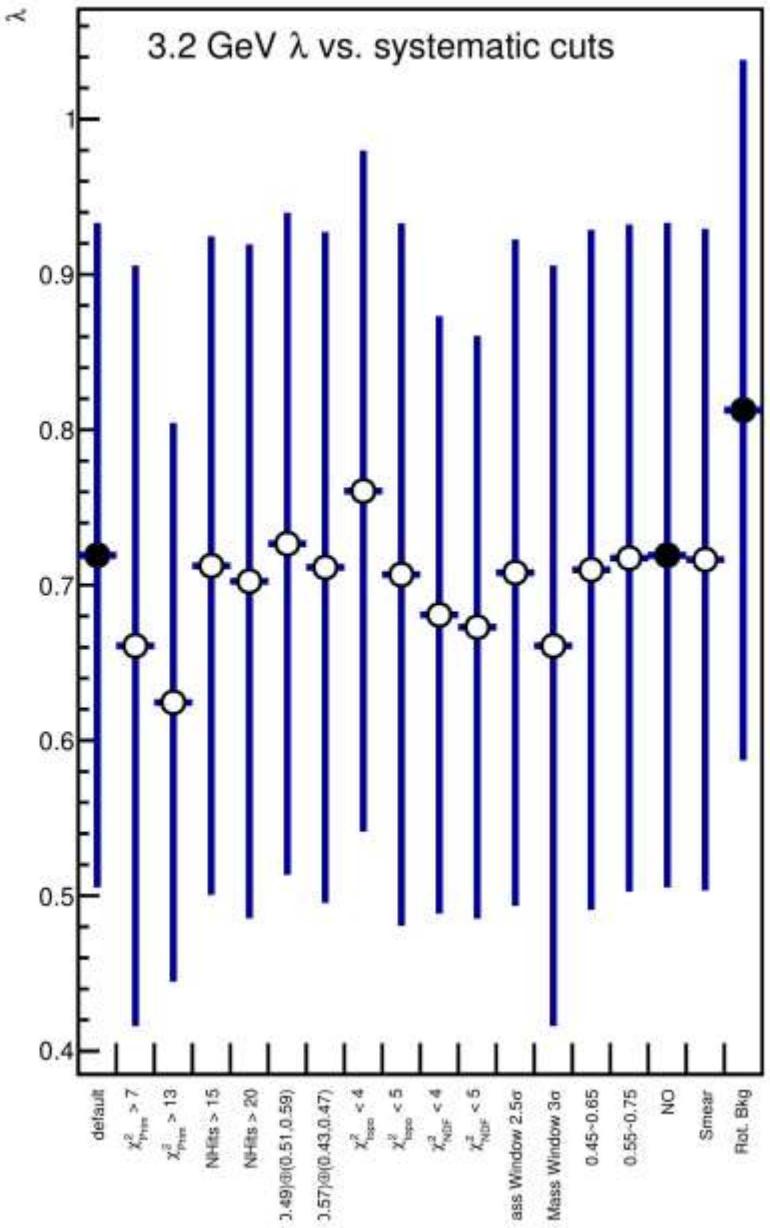

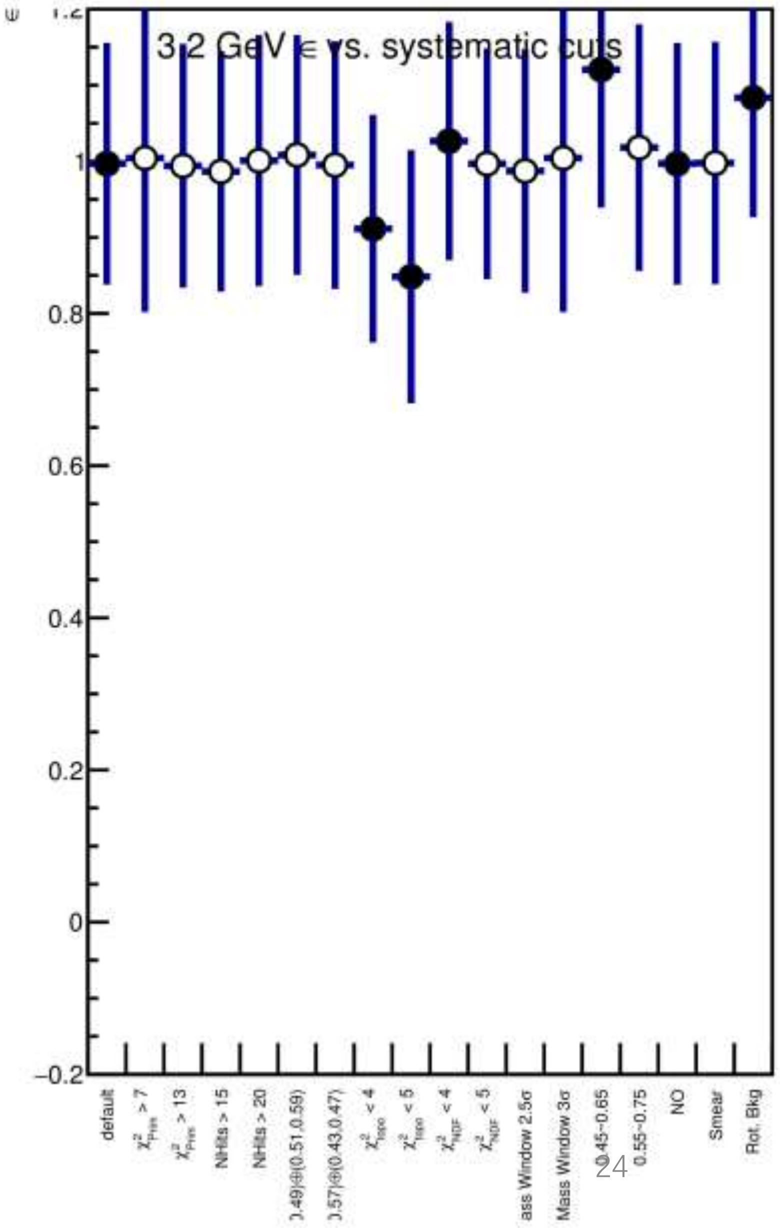

Systematic study

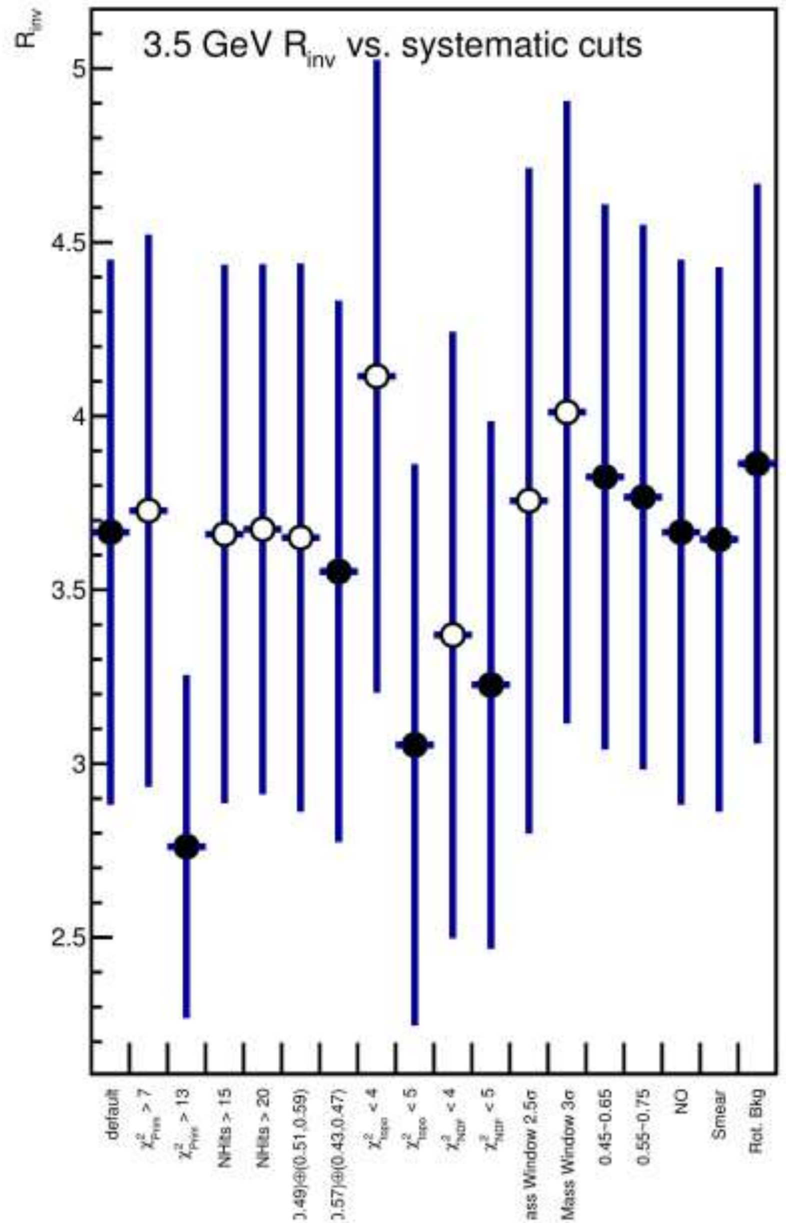

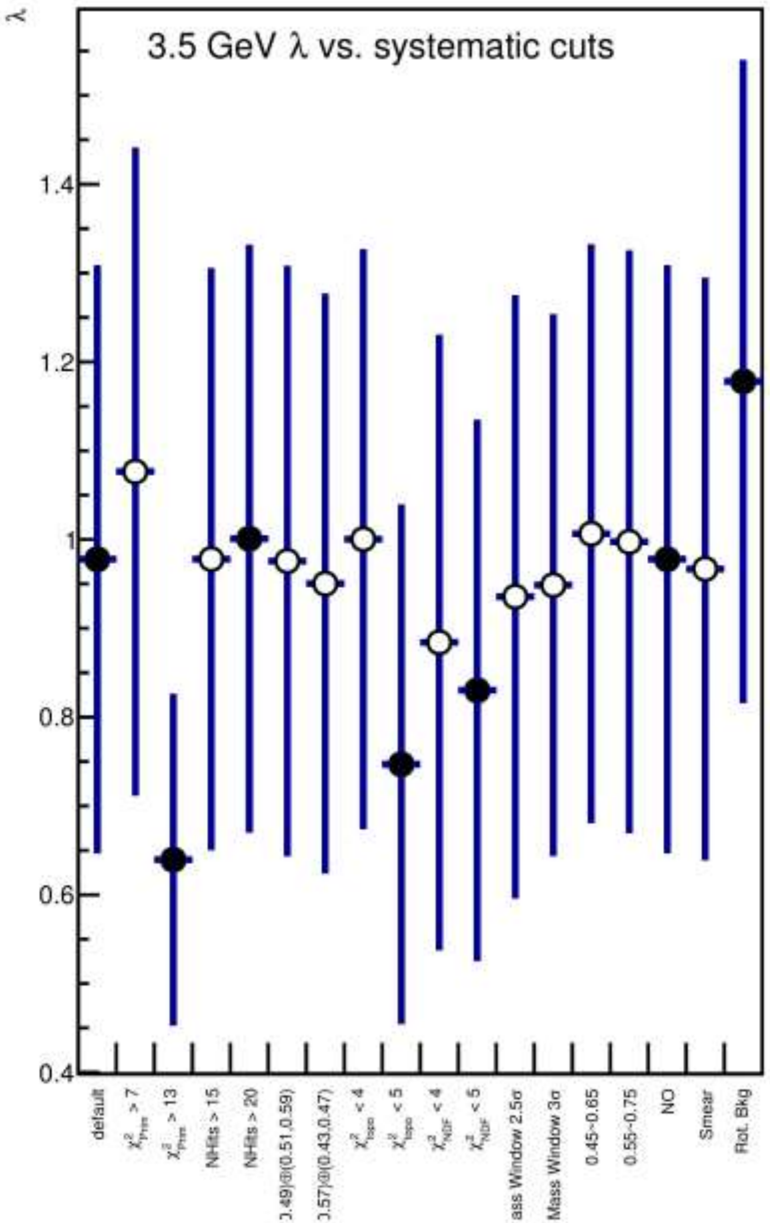

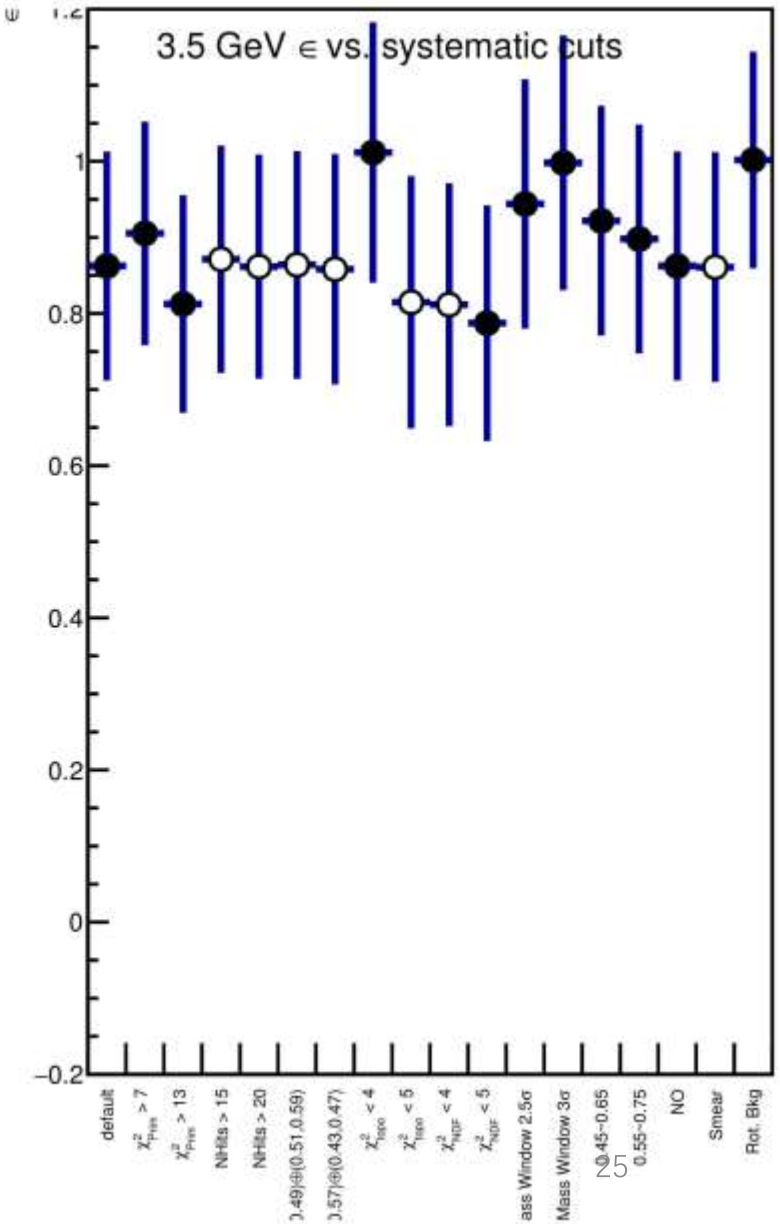

Systematic study

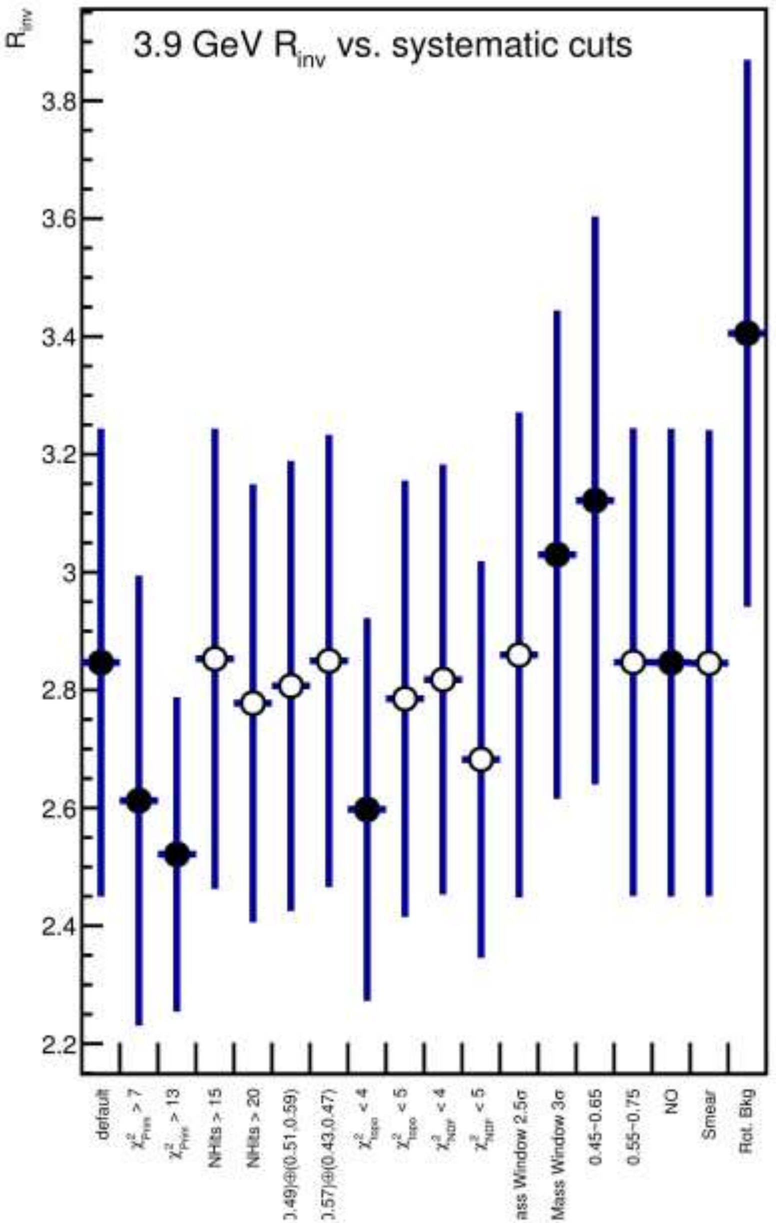

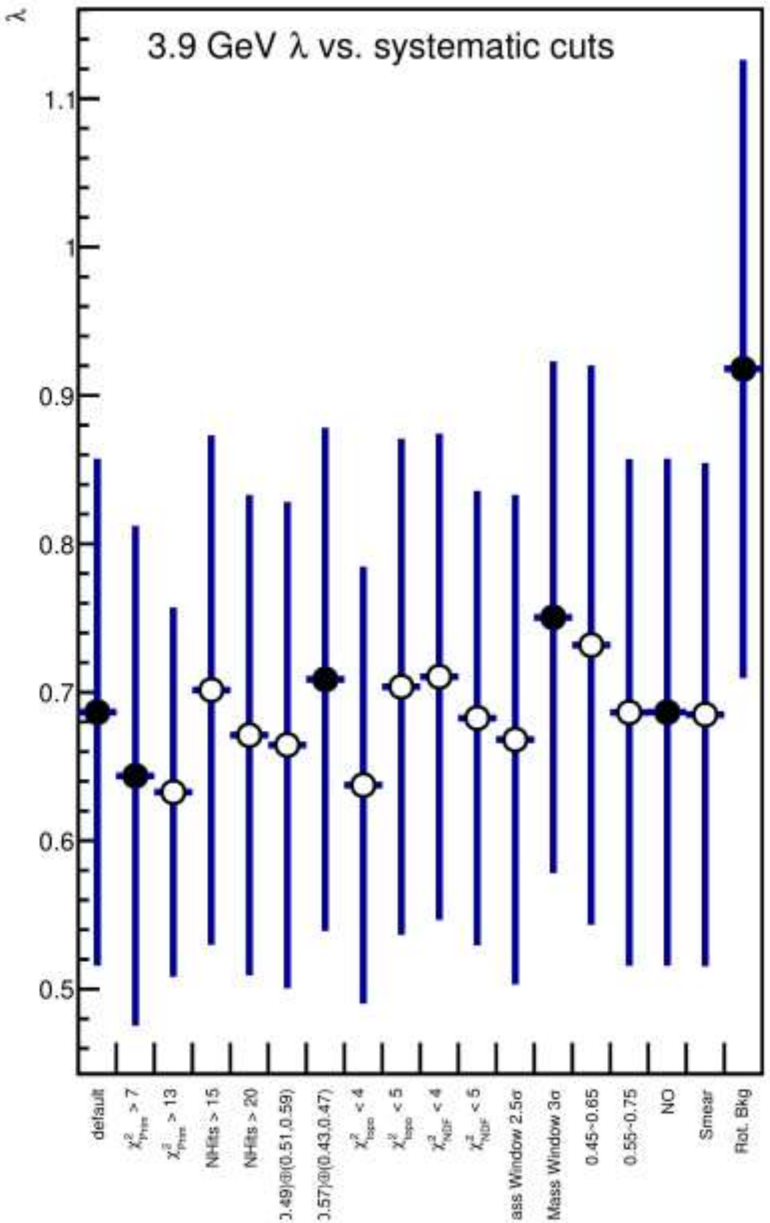

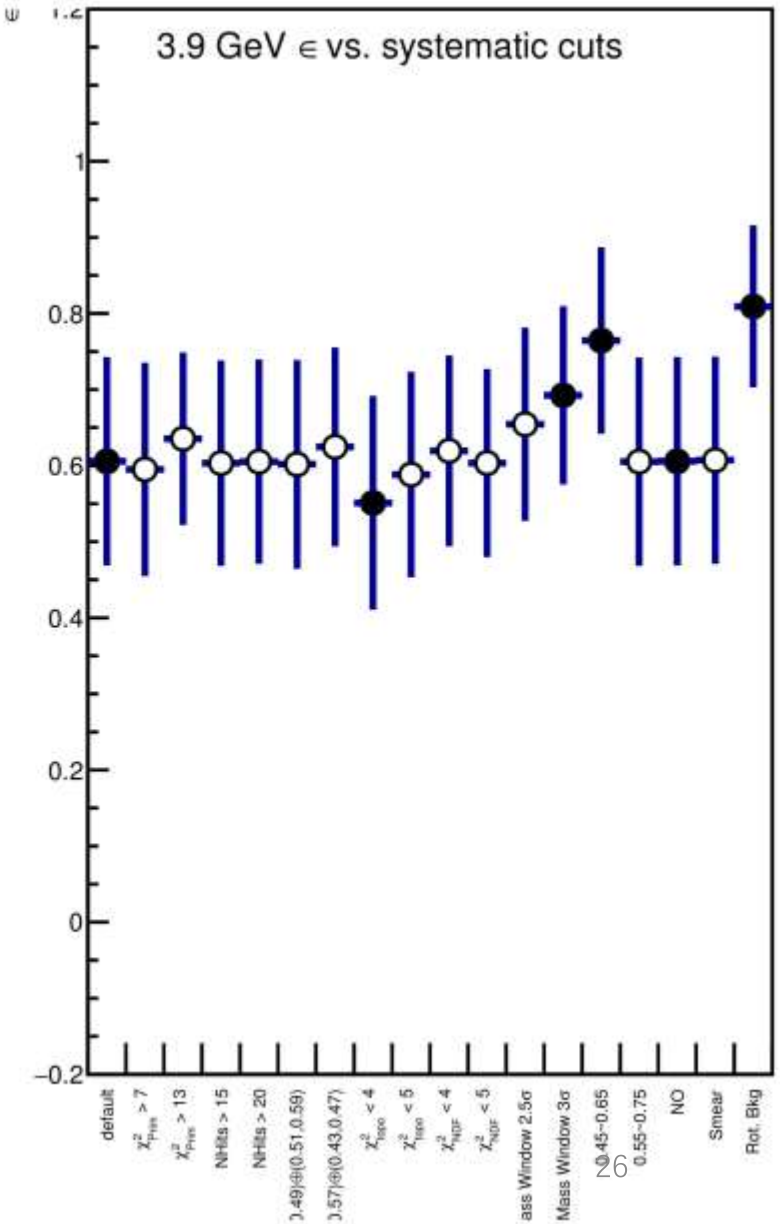

Systematic study

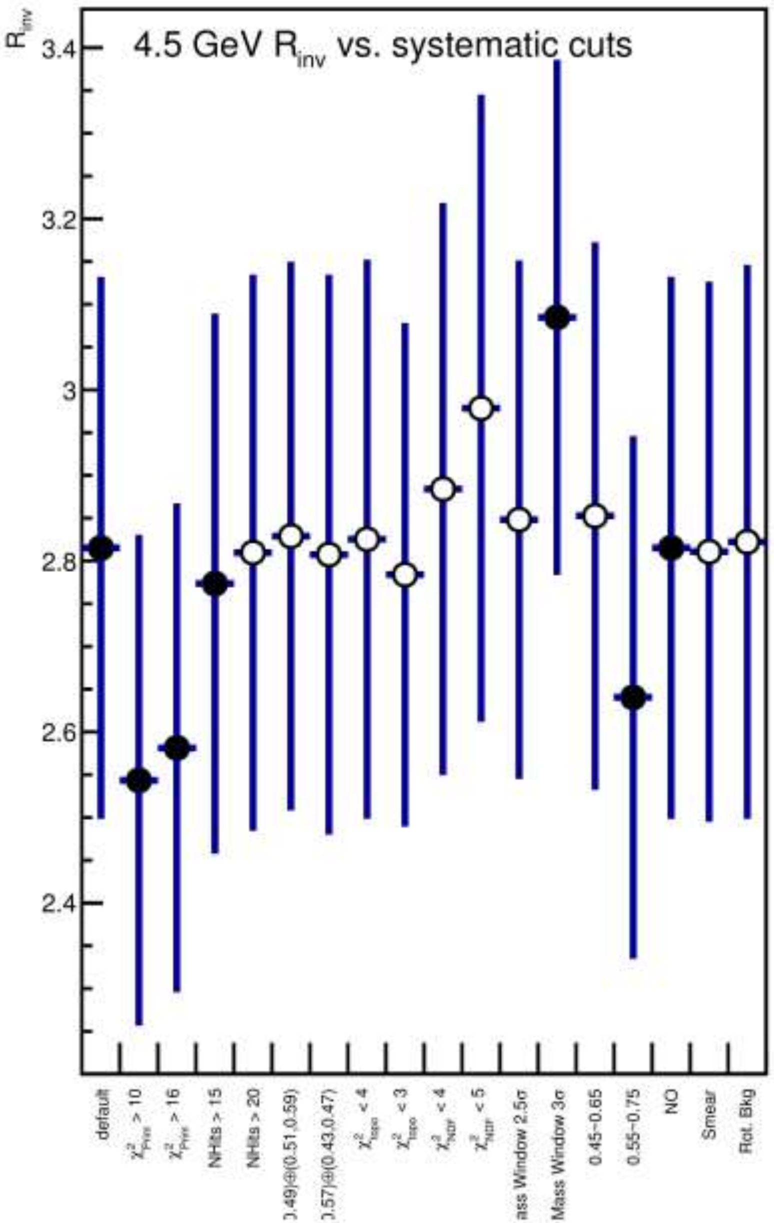

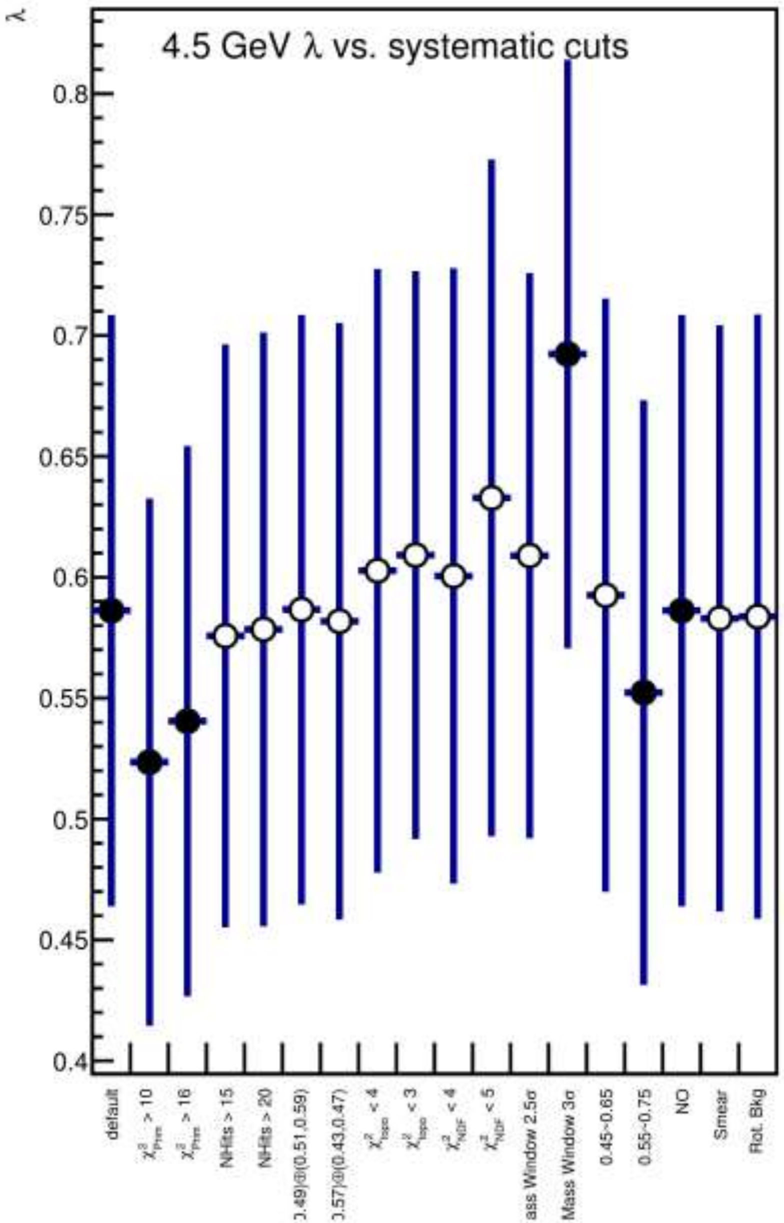

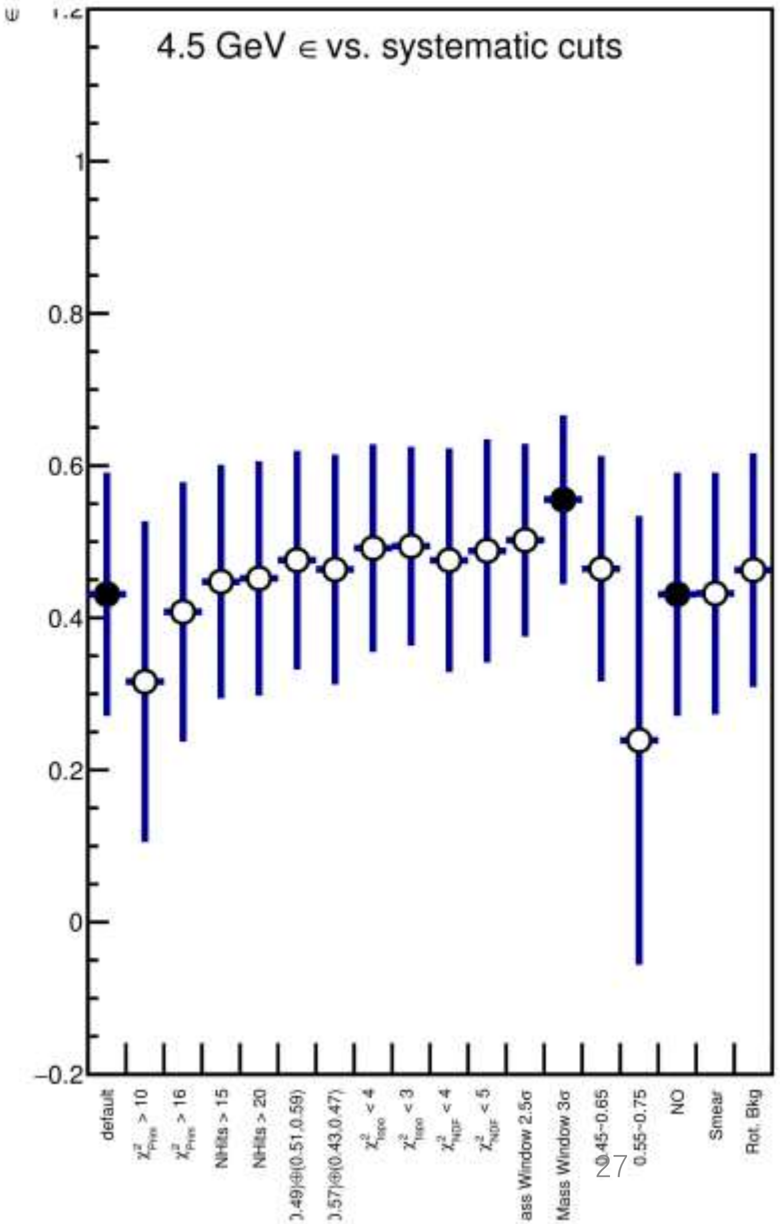

Systematic contribution of $K_s^0 K_s^0$

3.0 GeV	Rinv	lambda	epsilon
NHitsFit	0	0	0
$\chi^2_{prim\ \pi^{\pm}}$	0	0	46.72%
χ^2_{NDF}	0	10.99%	0
χ^2_{Topo}	0	0	9.75%
Mass window	0	7.66%	0
Side Band range	0	0	0
Background estimate method	0	0	28.28%
Fitting range	9.31%	29.73%	0
Normalize Range	0	0	0
Momentum correction	0	0	0
total	9.31%	32.61%	55.48%

Systematic contribution of $K_s^0 K_s^0$

3.2 GeV	Rinv	lambda	epsilon
NHitsFit	0	0	0
$\chi^2_{prim\ \pi^\pm}$	6.95%	0	0
χ^2_{NDF}	0	0	0.92%
χ^2_{Topo}	0	0	11.02%
Mass window	0	0	0
Side Band range	0	0	0
Background estimate method	0	0	8.38%
Normalize Range	0	0	6.20%
Momentum correction	4.20%	8.34%	0
Total	8.12%	8.34%	15.19%

Systematic contribution of $K_s^0 K_s^0$

3.5 GeV	Rinv	lambda	epsilon
NHitsFit	0	1.39%	0
$\chi^2_{prim\ \pi^{\pm}}$	12.90%	14.43%	2.62%
χ^2_{NDF}	7.59%	5.14%	5.40%
χ^2_{Topo}	11.18%	12.39%	10.27%
Mass window	0	0	10.20%
Side Band range	1.47%	0	0
Background estimate method	1.96%	13.96%	15.12%
Normalize Range	3.56%	0	5.59%
Momentum correction	0.54%	0	0
total	19.18%	24.19%	22.48%

Systematic contribution of $K_s^0 K_s^0$

3.9 GeV	Rinv	lambda	epsilon
NHitsFit	0	0	0
$\chi^2_{prim\ \pi^\pm}$	6.22%	3.31%	0
χ^2_{NDF}	0	0	0
χ^2_{Topo}	2.50%	0	5.24%
Mass window	3.47%	6.12%	5.82%
Side Band range	0	0.85%	0
Background estimate method	17.72%	28.88%	30.45%
Normalize Range	0.78%	0	17.09%
Momentum correction	0	0	0
total	19.28%	29.72%	35.79%

Systematic contribution of $K_s^0 K_s^0$

4.5 GeV	Rinv	lambda	epsilon
NHitsFit	0.78%	0	0
$\chi^2_{prim\ \pi^{\pm}}$	7.61%	3.74%	0
χ^2_{NDF}	0	0	0
χ^2_{Topo}	0	0	0
Mass window	6.30%	12.72%	7.81%
Side Band range	0	0	0
Background estimate method	0	0	0
Normalize Range	3.84%	3.46%	0
Momentum correction	0	0	0
total	10.63%	13.70%	7.81%

Systematic contribution of K^+K^+

3.0 GeV	Rinv	lambda	3.2 GeV	Rinv	lambda
NHitsFit	0	0	NHitsFit	0	0
DCA	0	0	DCA	0	0.04%
$\|n\sigma\|$	5.16%	0	$\|n\sigma\|$	0	1.43%
$\|\Delta\phi^*\|$	1.21%	2.19%	$\|\Delta\phi^*\|$	0.86%	4.04%
$\|\Delta\theta\|$	0	2.62%	$\|\Delta\theta\|$	0.31%	0
Splitting level	0	0	Splitting level	0	0
TOF m^2	9.28%	0	TOF m^2	0	0
Momentum correction	0	0	Momentum correction	0.79%	0.37%
Fit range	2.72%	0	Fit range	1.21%	0
total	11.03%	3.41%	total	1.71%	4.30%

Systematic contribution of K^+K^+

3.5 GeV	Rinv	lambda	3.9 GeV	Rinv	lambda
NHitsFit	0	0	NHitsFit	0.03%	0
DCA	0.24%	0	DCA	0.29%	0.22%
$\|n\sigma\|$	0	0	$\|n\sigma\|$	0	0.57%
$\|\Delta\phi^*\|$	1.93%	2.41%	$\|\Delta\phi^*\|$	0.16%	1.07%
$\|\Delta\theta\|$	1.83%	1.56%	$\|\Delta\theta\|$	0.48%	3.45%
Splitting level	0	0	Splitting level	0	0.13%
TOF m^2	0	0	TOF m^2	0	0
Momentum correction	0.86%	0.38%	Momentum correction	0.73%	0.24%
Fit range	0	0	Fit range	0	0
total	2.81%	2.90%	total	0.93%	3.67%

Comparison of difference parameters

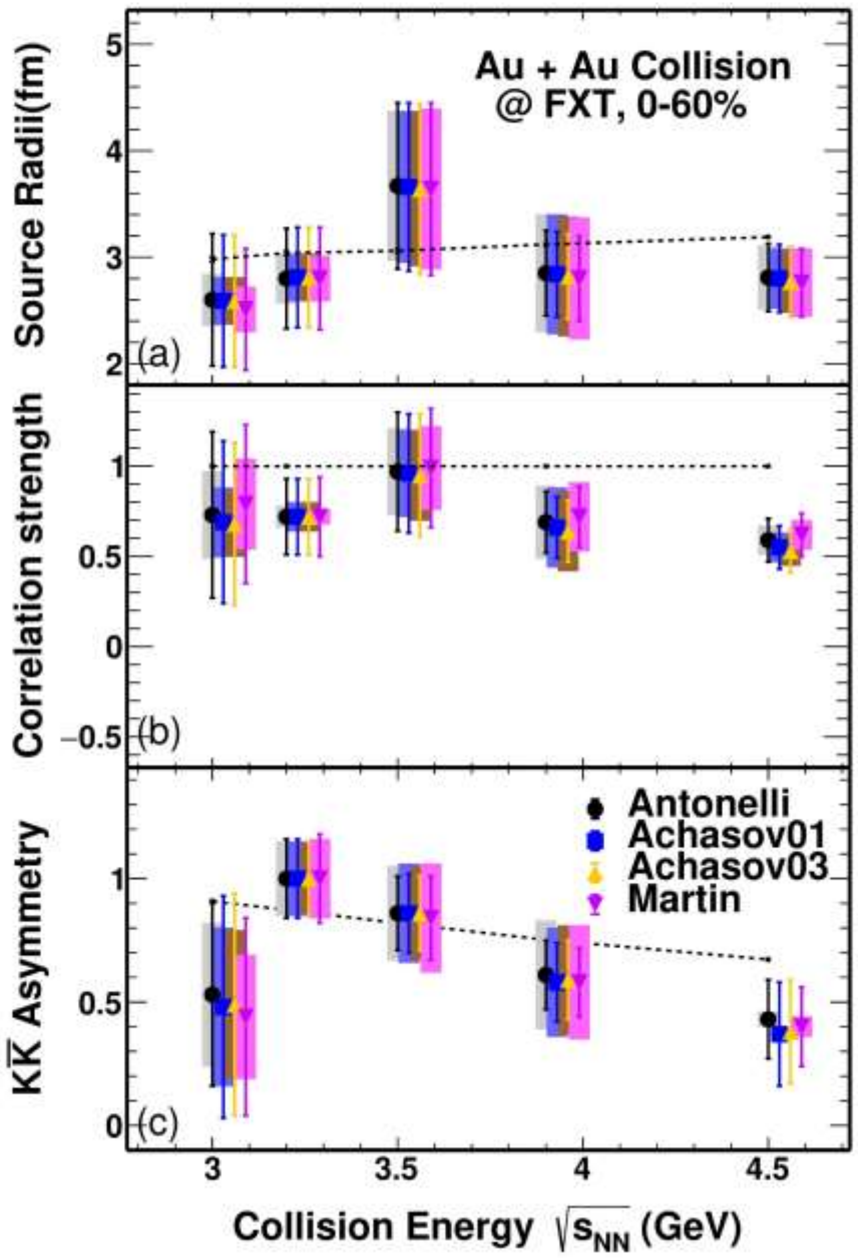

Antonelli	3.0 GeV	3.2 GeV	3.5 GeV	3.9 GeV	4.5 GeV
r_G (fm)	2.60±0.62±0.24	2.80±0.47±0.23	3.67±0.78±0.70	2.85±0.40±0.55	2.81±0.32±0.30
λ	0.73±0.46±0.24	0.72±0.21±0.06	0.97±0.33±0.24	0.69±0.17±0.20	0.59±0.12±0.08
ϵ	0.53±0.37±0.29	1.00±0.16±0.15	0.86±0.15±0.19	0.61±0.14±0.22	0.43±0.16±0.03
Achasov2001	3.0 GeV	3.2 GeV	3.5 GeV	3.9 GeV	4.5 GeV
r_G (fm)	2.59±0.62±0.22	2.81±0.47±0.22	3.66±0.79±0.71	2.84±0.40±0.56	2.80±0.32±0.28
λ	0.69±0.45±0.19	0.72±0.21±0.08	0.96±0.33±0.24	0.66±0.17±0.22	0.55±0.12±0.08
ϵ	0.48±0.45±0.32	1.00±0.16±0.15	0.86±0.16±0.20	0.58±0.16±0.22	0.37±0.21±0.00
Achasov2003	3.0 GeV	3.2 GeV	3.5 GeV	3.9 GeV	4.5 GeV
r_G (fm)	2.59±0.62±0.22	2.81±0.47±0.22	3.64±0.80±0.72	2.82±0.40±0.56	2.77±0.33±0.29
λ	0.68±0.45±0.18	0.72±0.21±0.08	0.95±0.34±0.25	0.64±0.17±0.22	0.53±0.12±0.08
ϵ	0.49±0.45±0.30	1.00±0.15±0.14	0.86±0.15±0.19	0.59±0.16±0.22	0.38±0.21±0.00
Martin	3.0 GeV	3.2 GeV	3.5 GeV	3.9 GeV	4.5 GeV
r_G (fm)	2.51±0.57±0.21	2.80±0.48±0.21	3.64±0.81±0.75	2.80±0.40±0.57	2.76±0.32±0.32
λ	0.79±0.44±0.25	0.72±0.22±0.04	0.99±0.33±0.23	0.72±0.17±0.19	0.62±0.12±0.08
ϵ	0.44±0.40±0.25	1.00±0.18±0.16	0.84±0.17±0.22	0.58±0.14±0.23	0.40±0.16±0.04

Pion 1-D CF

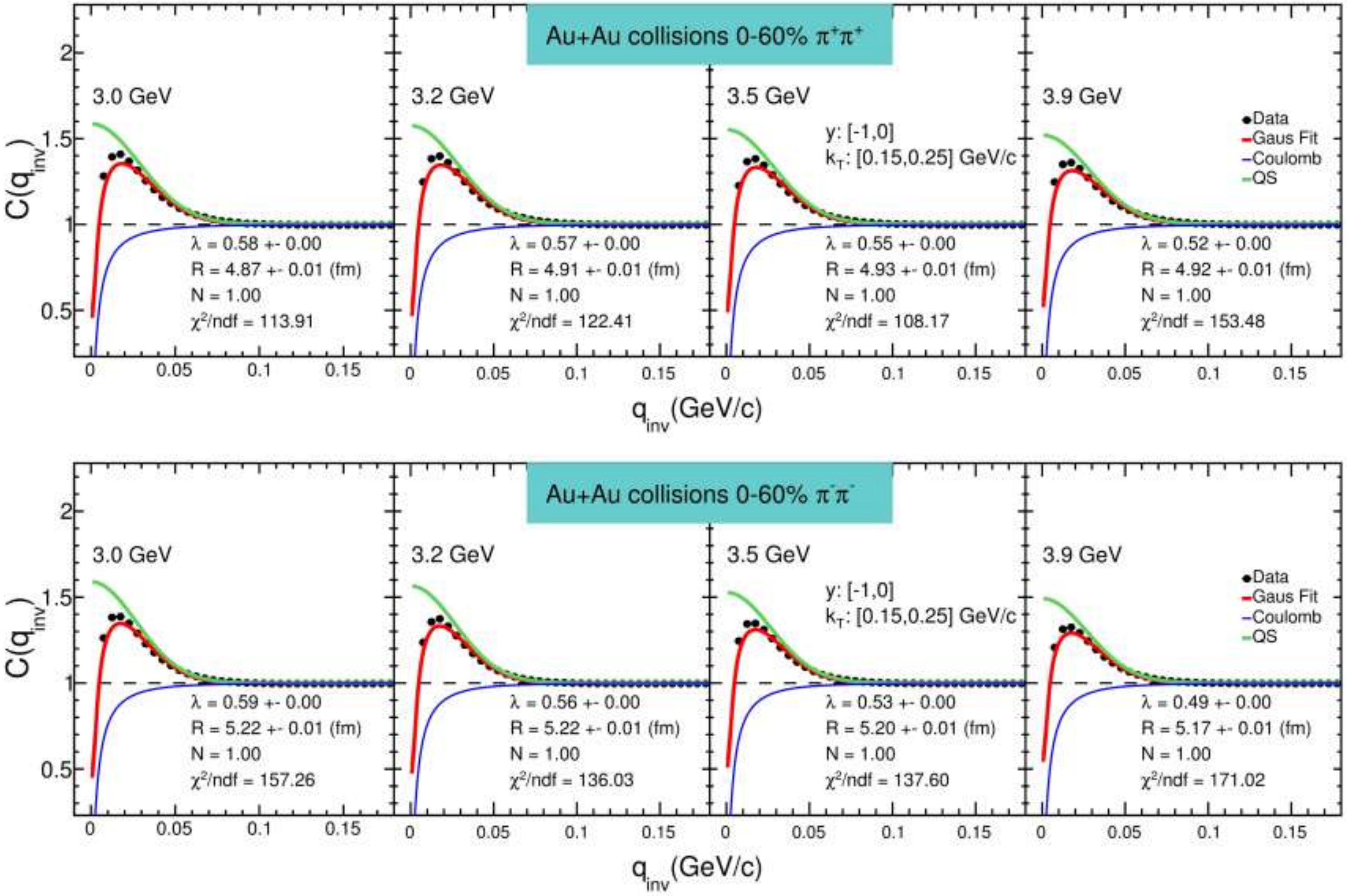

Au+Au collisions 0-60% π⁺π⁺
3.0 GeV
3.2 GeV
3.5 GeV
3.9 GeV
y: [-1,0]
k_T: [0.15,0.25] GeV/c
Data
Gaus Fit
Coulomb
QS
λ = 0.58 +- 0.00
R = 4.87 +- 0.01 (fm)
N = 1.00
χ²/ndf = 113.91
λ = 0.57 +- 0.00
R = 4.91 +- 0.01 (fm)
N = 1.00
χ²/ndf = 122.41
λ = 0.55 +- 0.00
R = 4.93 +- 0.01 (fm)
N = 1.00
χ²/ndf = 108.17
λ = 0.52 +- 0.00
R = 4.92 +- 0.01 (fm)
N = 1.00
χ²/ndf = 153.48
C(q_inv)
q_inv (GeV/c)
Au+Au collisions 0-60% π⁻π⁻
3.0 GeV
3.2 GeV
3.5 GeV
3.9 GeV
y: [-1,0]
k_T: [0.15,0.25] GeV/c
Data
Gaus Fit
Coulomb
QS
λ = 0.59 +- 0.00
R = 5.22 +- 0.01 (fm)
N = 1.00
χ²/ndf = 157.26
λ = 0.56 +- 0.00
R = 5.22 +- 0.01 (fm)
N = 1.00
χ²/ndf = 136.03
λ = 0.53 +- 0.00
R = 5.20 +- 0.01 (fm)
N = 1.00
χ²/ndf = 137.60
λ = 0.49 +- 0.00
R = 5.17 +- 0.01 (fm)
N = 1.00
χ²/ndf = 171.02
C(q_inv)
q_inv (GeV/c)

Pion 1-D CF

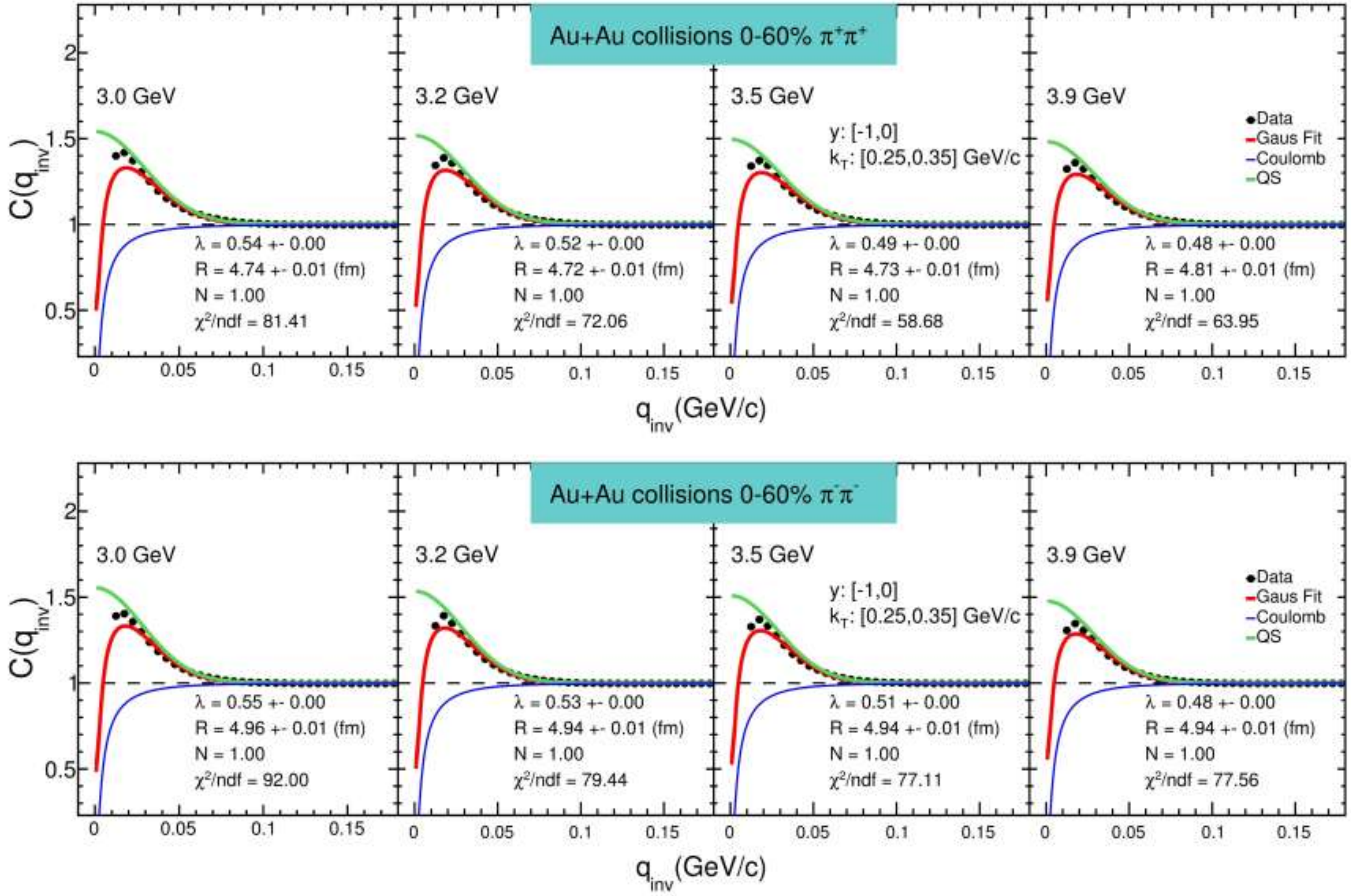
Au+Au collisions 0-60% $\pi^+\pi^+$
3.0 GeV
3.2 GeV
3.5 GeV
3.9 GeV
y: [-1,0]
k_T: [0.25,0.35] GeV/c
Data
Gaus Fit
Coulomb
QS
λ = 0.54 +- 0.00
R = 4.74 +- 0.01 (fm)
N = 1.00
χ^2/ndf = 81.41
λ = 0.52 +- 0.00
R = 4.72 +- 0.01 (fm)
N = 1.00
χ^2/ndf = 72.06
λ = 0.49 +- 0.00
R = 4.73 +- 0.01 (fm)
N = 1.00
χ^2/ndf = 58.68
λ = 0.48 +- 0.00
R = 4.81 +- 0.01 (fm)
N = 1.00
χ^2/ndf = 63.95
$C(q_{inv})$
q_{inv}(GeV/c)
Au+Au collisions 0-60% $\pi^-\pi^-$
3.0 GeV
3.2 GeV
3.5 GeV
3.9 GeV
y: [-1,0]
k_T: [0.25,0.35] GeV/c
Data
Gaus Fit
Coulomb
QS
λ = 0.55 +- 0.00
R = 4.96 +- 0.01 (fm)
N = 1.00
χ^2/ndf = 92.00
λ = 0.53 +- 0.00
R = 4.94 +- 0.01 (fm)
N = 1.00
χ^2/ndf = 79.44
λ = 0.51 +- 0.00
R = 4.94 +- 0.01 (fm)
N = 1.00
χ^2/ndf = 77.11
λ = 0.48 +- 0.00
R = 4.94 +- 0.01 (fm)
N = 1.00
χ^2/ndf = 77.56
$C(q_{inv})$
q_{inv}(GeV/c)

Pion 1-D CF

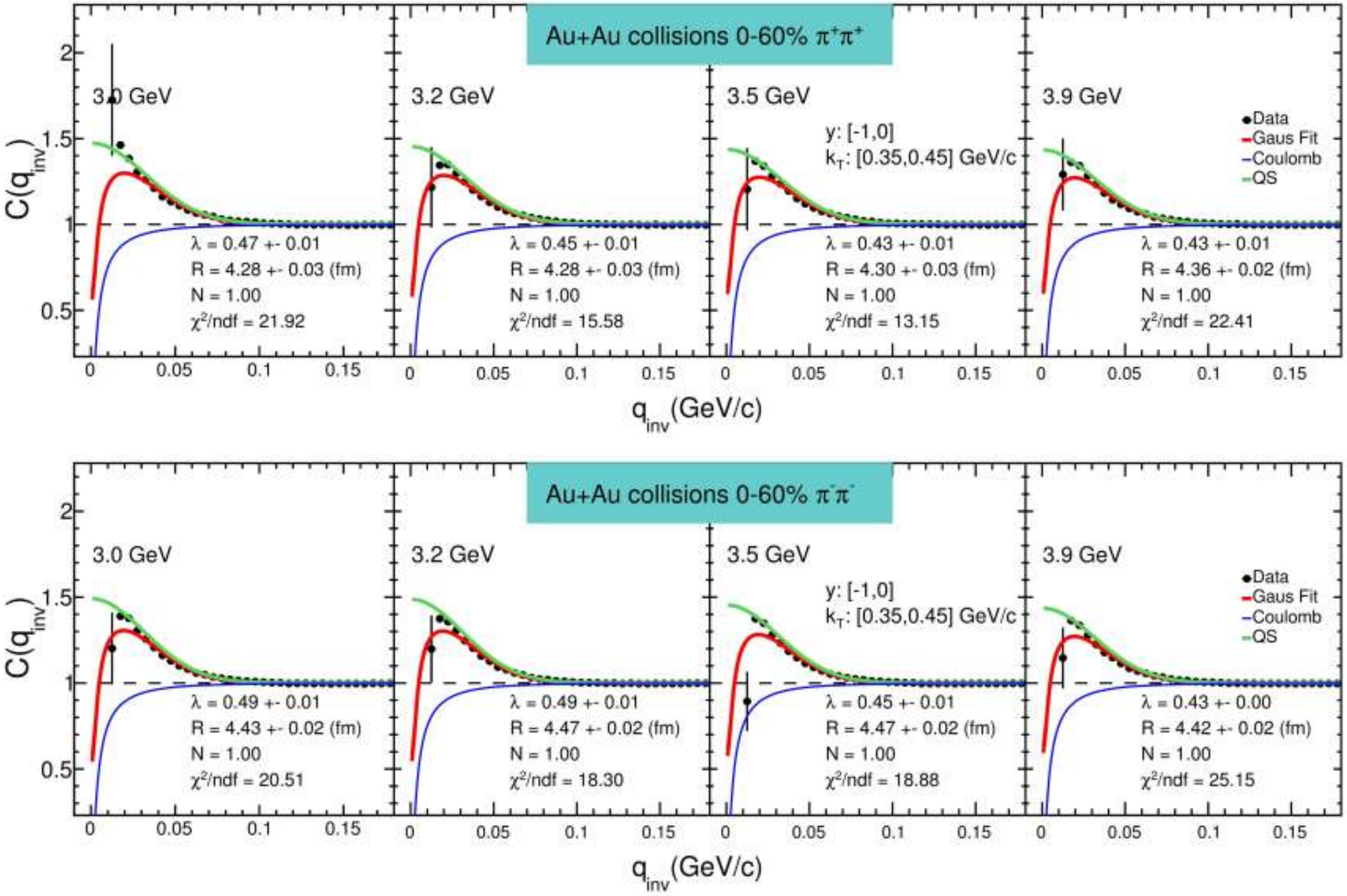

Au+Au collisions 0-60% π+π+
3.0 GeV
3.2 GeV
3.5 GeV
3.9 GeV
y: [-1,0]
kT: [0.35,0.45] GeV/c
Data
Gaus Fit
Coulomb
QS
λ = 0.47 +- 0.01
R = 4.28 +- 0.03 (fm)
N = 1.00
χ2/ndf = 21.92
λ = 0.45 +- 0.01
R = 4.28 +- 0.03 (fm)
N = 1.00
χ2/ndf = 15.58
λ = 0.43 +- 0.01
R = 4.30 +- 0.03 (fm)
N = 1.00
χ2/ndf = 13.15
λ = 0.43 +- 0.01
R = 4.36 +- 0.02 (fm)
N = 1.00
χ2/ndf = 22.41
C(qinv)
qinv(GeV/c)
Au+Au collisions 0-60% π-π-
3.0 GeV
3.2 GeV
3.5 GeV
3.9 GeV
y: [-1,0]
kT: [0.35,0.45] GeV/c
Data
Gaus Fit
Coulomb
QS
λ = 0.49 +- 0.01
R = 4.43 +- 0.02 (fm)
N = 1.00
χ2/ndf = 20.51
λ = 0.49 +- 0.01
R = 4.47 +- 0.02 (fm)
N = 1.00
χ2/ndf = 18.30
λ = 0.45 +- 0.01
R = 4.47 +- 0.02 (fm)
N = 1.00
χ2/ndf = 18.88
λ = 0.43 +- 0.00
R = 4.42 +- 0.02 (fm)
N = 1.00
χ2/ndf = 25.15
C(qinv)
qinv(GeV/c)

Pion 1-D CF

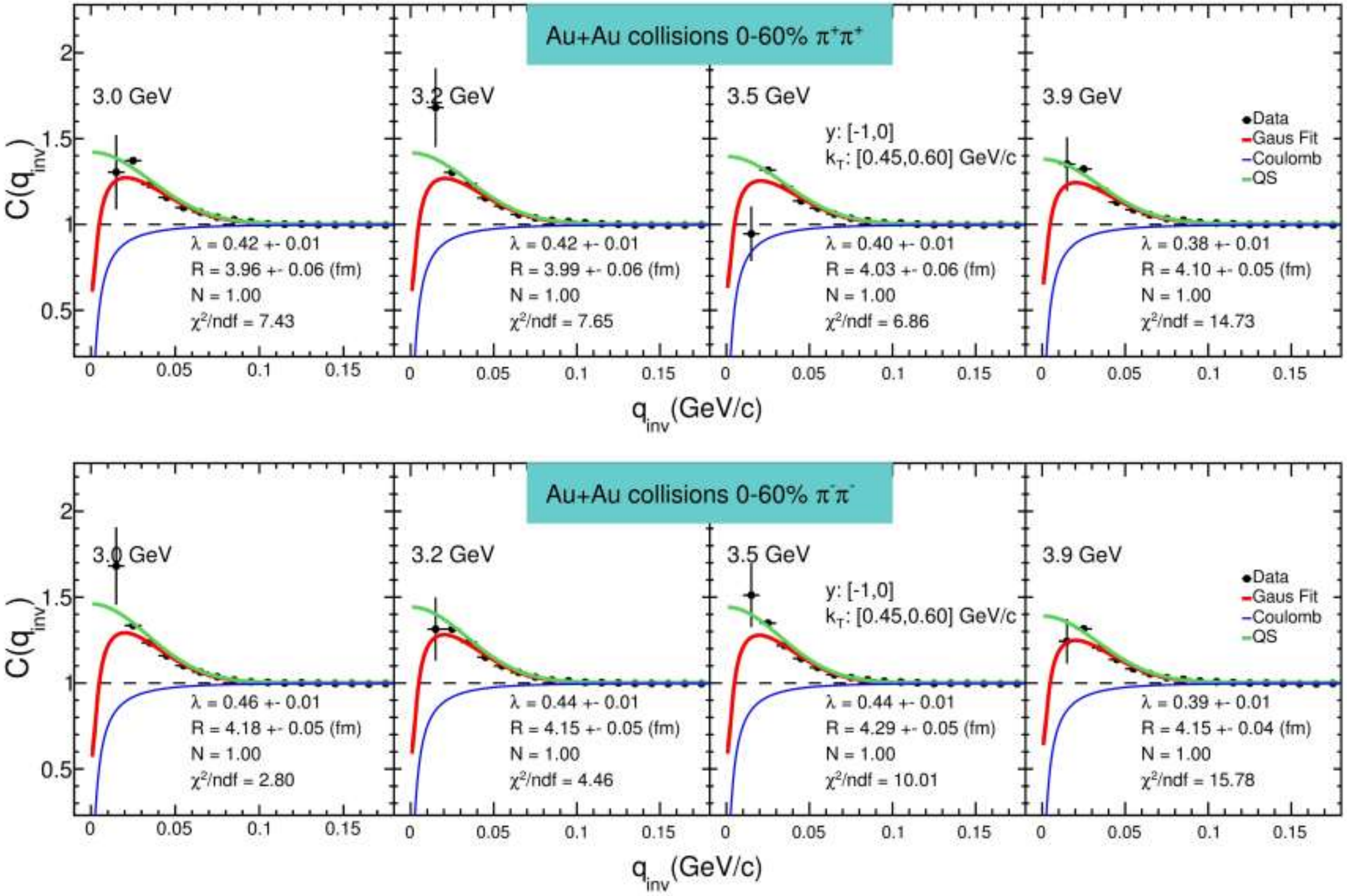

Au+Au collisions 0-60% $\pi^+\pi^+$
3.0 GeV
3.2 GeV
3.5 GeV
3.9 GeV
y: [-1,0]
k_T: [0.45,0.60] GeV/c
Data
Gaus Fit
Coulomb
QS
λ = 0.42 +- 0.01
R = 3.96 +- 0.06 (fm)
N = 1.00
χ^2/ndf = 7.43
λ = 0.42 +- 0.01
R = 3.99 +- 0.06 (fm)
N = 1.00
χ^2/ndf = 7.65
λ = 0.40 +- 0.01
R = 4.03 +- 0.06 (fm)
N = 1.00
χ^2/ndf = 6.86
λ = 0.38 +- 0.01
R = 4.10 +- 0.05 (fm)
N = 1.00
χ^2/ndf = 14.73
$C(q_{inv})$
q_{inv}(GeV/c)
Au+Au collisions 0-60% $\pi^-\pi^-$
3.0 GeV
3.2 GeV
3.5 GeV
3.9 GeV
y: [-1,0]
k_T: [0.45,0.60] GeV/c
Data
Gaus Fit
Coulomb
QS
λ = 0.46 +- 0.01
R = 4.18 +- 0.05 (fm)
N = 1.00
χ^2/ndf = 2.80
λ = 0.44 +- 0.01
R = 4.15 +- 0.05 (fm)
N = 1.00
χ^2/ndf = 4.46
λ = 0.44 +- 0.01
R = 4.29 +- 0.05 (fm)
N = 1.00
χ^2/ndf = 10.01
λ = 0.39 +- 0.01
R = 4.15 +- 0.04 (fm)
N = 1.00
χ^2/ndf = 15.78
$C(q_{inv})$
q_{inv}(GeV/c)

Table 2: resonance mass extraction

	Parameters	3.0 GeV	3.2 GeV	3.5 GeV	3.9 GeV	4.5 GeV
$K_s^0 - K_s^0$	r_G(fm)	3.02±0.91 ±0.89	2.62±0.37 ±0.26	3.91±0.69 ±0.89	3.08±0.38 ±0.0.31	3.11±0.29 ±0.16
	λ	0.73±0.60 ±0.21	0.71±0.21 ±0.08	1.06±0.34 ±0.29	0.78±0.18 ±0.08	0.68±0.13 ±0.05
	Gaus. fitting r_G(fm)	3.15±1.07 ±0.00	2.81±0.39 ±0.10	4.30±0.67 ±0.52	3.86±0.52 ±0.22	3.91±0.38 ±0.08
	Gaus. fitting λ	0.65±0.54 ±0.02	0.72±0.21 ±0.00	1.09±0.31 ±0.03	0.81±0.21 ±0.02	0.66±0.13 ±0.01
	ϵ	0.91	0.87	0.82	0.75	0.67
	m_{f_0}(MeV/c^2)	945.73±72.90 ±00.00		m_{a_0}(MeV/c^2)	986.04±55.21 ±00.00